REPUBLIC OF TURKEY

ACIBADEM MEHMET ALİ AYDINLAR UNIVERSITY

INSTITUTE OF NATURAL AND APPLIED SCIENCES

Genetic Research in Autoinflammatory Diseases

ZEYNEP TONBUL

MASTER THESIS

DEPARTMENT OF MOLECULAR AND TRANSLATIONAL BIOMEDICINE

SUPERVISOR

Prof.Eda Tahir Turanlı

SECOND SUPERVISOR

Asst. Prof. Dr. Umut İnci Onat

ISTANBUL-2024

REPUBLIC OF TURKEY

ACIBADEM MEHMET ALİ AYDINLAR UNIVERSITY

INSTITUTE OF NATURAL AND APPLIED SCIENCES

Genetic Research in Autoinflammatory Diseases

ZEYNEP TONBUL

MASTER THESIS

DEPARTMENT OF MOLECULAR AND TRANSLATIONAL BIOMEDICINE

SUPERVISOR

Prof.Eda Tahir Turanlı

SECOND SUPERVISOR

Asst. Prof. Dr. Umut İnci Onat

ISTANBUL-2024

DECLARATION

I declare that this thesis work is my own work; I had no unethical behavior at any stages from the planning to the writing of the thesis, I obtained all the information in this thesis in accordance with academic and ethical rules, I cited all the information and comments that were not obtained with this thesis work, and I provided resources in the list of references. I also declare that there was no violation of any patents and copyrights during the study and writing of this thesis.

Zeynep Tonbul

PREFACE AND ACKNOWLEDGEMENTS

I want to begin by conveying my sincere appreciation to my advisor, Prof. Eda Tahir Turanlı, for her unwavering support, motivation, patience, and extensive knowledge. Throughout the entire process of researching and writing this thesis, her guidance has been invaluable. I am truly grateful to have had such an exceptional advisor and mentor during my MSc .studies.

Secondly, I would like to express my sincere gratitude to my co-advisor Asst. Prof. Dr. Umut İnci Onat. She always supported and motivated me in every situation. She was always there with a solution when I doubted myself, struggling against errors. Without her guidance, I would not reveal my capabilities in our work.

I cannot forget my fellow labmates Gülipek Güven, Umut Voyvoda, Fatma Coşkun, and Batuhan Savsar for their support and friendship in my academic and personal life. Together, we brainstormed to solve challenging issues and conduct tough and exhausting experiments within our projects. Additionally, I would like to thank my close friends for their precious and amazing friendship in the best and worst times of my life.

My biggest and special gratitude goes to my beloved parents, my mother Seher , my father Zekeriya and my sisters, Begüm Tonbul , Elif Tonbul and Elçin Tonbul for their love, endless support and patience through my whole life. If I would not have them as my parents , I could not be the person who I am now. They always supported me in my every decision. I love you with all my heart and we will always love each other forever.

This thesis has been supported by the Scientific Research Projects Commission Presidency of Acıbadem Mehmet Ali Aydınlar University with project number 14 and project number 21.

Lastly, I want to thank myself for the dedication, determination, and countless hours invested in this journey. I take pride in myself and what I have accomplished.

Zeynep Tonbul

TABLE OF CONTENTS

Page

LIST OF ABBREVIATIONS AND SYMBOLS

Ab	Antibody
ATP	Adenosine Triphosphate
ASC	Adapter protein apoptosis-associated speck-like protein containing a CARD
APS	Ammonium persulfate
BSA	Bovine serum albumin
Bp	Base pair
$CaCI_2$	Calcium chloride
DAMPs	Danger-Associated Molecular Patterns
DNA	Deoxyribonucleic Acid
dsDNA	Double Strand DNA
ddH_2O	double-distilled water
DMSO	Dimethyl sulfoxide
E.coli	Escherichia coli
ECL	Enhanced Chemiluminescence
EDTA	Ethylenediaminetetraacetic Acid
FBS	Fetal Bovine Serum
FMF	Familial Mediterranean fever
GAPDH	Glyceraldehyde-3-Phosphate Dehydrogenase
HEPES	4-(2-Hydroxyethyl)-1-Piperazineethanesulfonic Acid
HLA	Human Leukocyte antigen
HRP	Horseradish Peroxidase

IL-1	Interleukin 1
IL-1B	Interleukin 1- Beta
IL-6	Interleukin 6
IFN-γ	Interferon gamma
LB	Luria Bertani
LPS	Lipopolysaccharides
$MgCI_2$	Magnesium Chloride
Mt	Mutant
MLX	Max-like protein X
NCBI	National Center for Biotechnology Information
NK	Natural Killer
NLRP3	Nucleotide-binding domain, leucine-rich–containing family, pyrin domain–containing-3
NTC	Negative Control
PAMP	Pathogen-Associated Molecular Patterns
PAPA	Pyogenic Arthritis, Pyoderma gangrenosum, and Acne
PBS	Phosphate Buffered Saline
PBST	Phosphate Buffered Saline- Tween
PCR	Polymerase chain reaction
PDGF	Platelet-derived growth factor
PRR	Pattern Recognition Receptor
PMA	Phorbol 12-myristate 13-acetate
PPP1R32	Protein Phosphatase 1 Regulatory Subunit 32
PSTPIP1	Proline-Serine-Threonine Phosphatase Interacting Protein 1

Pen-Strep	Penicillin-Streptomycin
PTP-PEST	Protein tyrosine phosphatase
RNA	Ribonucleic acid
RPMI	Roswell Park Memorial Institute
RT	Room temperature
SDS	Sodium dodecyl sulftate
SNP	Single nucleotide polymorphism
TA	Takayasu Arteritis
TAE	Tris-Acetate EDTA
TBS	Tris Buffered Saline
TBST	Tris Buffered Saline Tween
Th	Helper T cell
WB	Western Blot
WT	Wild type

LIST OF FIGURES

LIST OF TABLES

ABSTRACT

Autoinflammatory diseases, characterized by systemic inflammation and linked to the innate immune system, are induced by inflammasomes, with the development of autoinflammatory syndromes associated with the abnormal functioning of the innate immune system. One example for autoinflammatory disease is Familial Mediterranean Fever (FMF). Familial Mediterranean Fever is recognized as a prominent hereditary monogenic autoinflammatory disorder inherited in an autosomal recessive way. Individuals with FMF often undergo inflammation in the peritoneum, lungs and joints with episodes of fever. *MEFV* gene encodes a protein called pyrin. Pyrin protein has a crucial role in regulating innate immune response and fighting with infection. Mediterranean Fever occurs because of the pathogenic variants in the *MEFV* gene, and the pathogenic variants can impair the function of the pyrin protein, which IL1B level (pro-inflammatory cytokine) is increased. Nonetheless, around 15-20% of patients show no pathogenic variations in the *MEFV* gene. Subsequently, a study conducted by our gruop uncovered that a family traversing three ages presents an autoinflammatory phenotype appearing to be FMF; However, the patients do not have any *MEFV* gene pathogenic variants that could cause disease. The study demonstrated that two rare pathogenic variants (p.Arg228Cys and Ala372Val) in the *PSTPIP1* gene could contribute to the FMF phenotype. Thus, the initial part of this thesis aims to explore the effects and functional roles of these two rare missense pathogenic variants (p.R228C and p.A372V) on the pyrin inflammasome through *in vitro* cell culture models. To research the effects of the two pathogenic variants, site-directed mutagenesis is performed successfully for introducing specific nucleotide substitution (c.682C>T and c.1115C>T) within a vector which is PSTPIP1 cDNA cloned into it. Afterward, the THP-1 cell line is differentiated into macrophages by PMA to investigate the effects of the variants in cell culture. To create the inflammasome complex in cell culture, specified concentration of LPS and ATP were given to the THP-1 cells. The level of inflammasome markers, which are cleaved caspase-1 and mature IL1B, were examined by western blotting.

In the second part of the thesis, the aim is to investigate the potential role of the p.G200S (NM_145017.3: c.598G>A, rs148713373) missense variant in the *PPP1R32* gene, which is found in individuals diagnosed with TA from a family, using an in vitro cell culture model in the inflammasome. Takayasu Arteritis is a rare systemic inflammatory disease which medium and large arteries are affected by inflammation.

This thesis studies two consanguineous families exhibiting multiple affected individuals within the same generation to find a candidate gene for Takayasu Arteritis. The first TA family composed of healthy mother, father, and a younger brother with 2 sisters are affected. The second TA family resembles the first family, while two children out of three are affected. First, gene and variant filtration was performed according to the exome data of the two families. The filtration was done according to minor allele frequency (MAF<0.01), variant effect prediction software (CADD,PolyPhen,Mutation Taster) and also impact of the variant. Based on the variant filtration, c.598G>A and c.347G>A missense variants found on *PPP1R32* gene was selected to study. Afterwards, Sanger sequencing was performed for the variants to study further. Consequently, c.598G>A variant remained as candidate because of presenting as heterozygous status at individual TA1-03 and TA1-04, diagnosed with Takayasu Arteritis. Healthy controls (TA1-02 and TA1-05) were homozygous wild-type for c.598G>A variant. Additionally, this variant was homozygous wild-type for individual TA2-01 and TA2-02. Moreover, TA1-03 and TA1-04 diagnosed with TA was heererozygous status for c.347G>A. However, c.347G>A variant was eliminated because of presenting as heterozygous status at individual TA1-02, a healthy control. As a result of the sanger sequencing results, c.598G>A variant in *PPP1R32* gene was considered for further analysis. . To research the effects of the pathogenic variants, site-directed mutagenesis is performed successfully for introducing specific nucleotide substitution (c.598G>A) within a vector which is PPP1R32 cDNA cloned into it. Afterward, the THP1 cell line is differentiated into macrophages by PMA to investigate the effects of the variants in cell culture. Afterwards, wild type and mutant plasmid DNA were transfected to the THP-1 cells by using a lipid-based method. The level of inflammasome markers, which are cleaved caspase-1 and mature IL1B, were examined by western blotting.

Keywords: FMF, TA, Inflammasome, Cell Culture, IL1B, Caspase-1

ÖZET

Otoenflamatuar hastalıklar, öncelikle inflamazomlar tarafından tetiklenen sistemik inflamasyon ile karakterize edilir ve doğuştan gelen bağışıklık sistemi ile ilişkilidir. Otoenflamatuar sendromların gelişimi, doğuştan gelen bağışıklık sisteminin anormal işleyişi ile bağlantılıdır. Otoenflamatuar hastalıklardan en yaygın olanı, Ailevi Akdeniz Ateşi hastalığıdır (AAA). Ailevi Akdeniz Ateşi, önde gelen kalıtsal monojenik otoenflamatuar bozukluk olarak kabul edilir ve otozomal resesif bir şekilde aktarılır. AAA'lı bireyler genellikle karın zarı, akciğerler ve eklemlerde inflamasyon yaşarlar ve ateş nöbetleri geçirirler. Hastalığın geni *MEFV* genidir. MEFV geni pirin adı verilen bir protein kodlar. Pirin proteini, doğuştan gelen bağışıklık yanıtını düzenlemede ve enfeksiyonla mücadelede kritik bir rol oynar. Ailese Akdeniz Ateşi, *MEFV* genindeki patojenik varyantlardan kaynaklanır ve bu patojenik varyantlar, pirin proteininin fonksiyonun bozup, proinflamatuar sitkoin olan IL1B'nın (İnterlökin 1-Beta) expressiyonu artabilir. Yapılan çalışmalara göre, hastaların yaklaşık %15-20'sinde *MEFV* geninde herhangi bir patojenik varyant bulunmamaktadır. Bu nedenle, son bir çalışma, üç nesildir devam eden bir ailenin AAA'ya benzeyen otoenflamatuar bir fenotip sergilediğini ancak hastalar, *MEFV* geninde herhangi bir patojenik varyant taşımamaktadır. Çalışma, PSTPIP1 genindeki iki nadir patojenik varyantın (p.R228C ve A372V) AAA fenotipine katkıda bulunabileceğini gösterdi. Bu nedenle, tezin ilk bölümü, bu iki nadir yanlış anlamlı patojenik varyantın (p.R228C ve p.A372V) pirim inflamazomu üzerindeki etkilerini ve işlevsel rollerini in vitro hücre kültürü modelleri aracılığıyla araştırmayı amaçlamaktadır. İki patojenik varyantın etkilerini araştırmak amacıyla, bu varyantlar için bölgeye yönlendirilmiş mutagenez başarıyla gerçekleştirildi. Mutagenez *PSTPIP1* geninin klonlandığı spesifik vektöre spesifik nükleotid değişimler yapıldı (c.682C>T ve c.1115C>T). Daha sonra, THP1 hücre hattı, varyantların hücre kültüründeki etkilerini incelemek için PMA kullanılarak makrofaja farklılaştırıldı. Daha sonra, hücre kültüründe pirin inflamazomu oluşturulmuştur. Böylece, aktif kaspaz-1 ve aktif IL1B gibi inflamazom belirteçlerinin seviyeleri, western blot analizi ile incelendi.

Tezin ikinci bölümünde, bir ailede TA teşhisi konmuş çok sayıda etkilenen bireyde bulunan *PPP1R32* genindeki p.G200S (NM_145017.3: c.598G>A, rs148713373) yanlış anlamlı varyantın ,in vitro hücre kültürü modeli kullanılarak inflamazomda potansiyel rolünü araştırmak amaçlanmaktadır. Takayasu Arteriti, orta ve büyük arterlerin iltihap nedeniyle etkilendiği nadir görülen sistemik bir iltihabi hastalıktır. Bu tezde, aynı nesilde birden fazla etkilenen birey içeren akraba evliliği olan aileler incelenerek Takayasu Arteriti hastalığının patojenezisi için aday bir gen bulunmaya çalışılmıştır. İlk TA ailesinde sağlıklı bir anne, baba ve erkek kardeş bulunurken, iki kız kardeş bu hastalıktan etkilenmiştir. İkinci TA ailesi, anne ve baba sağlıklıyken, üç çocuktan ikisi hastalıktan etkilenmiştir. Ekzom verilerini kullanarak gen ve varyant filtreleme yapılmış olup, *PPP1R32* genindeki c.598G>A ve c.347G>A varyantları ailedeki sağlıklı bireyler ve hastalara sanger sekanslama yapılmıştır. Sanger sonuçlarına göre, c.598G>A varyantı, Takayasu Arteriti teşhisi konmuş bireylerden TA1-03 ve TA1-04'te heterozigot durumda bulunması nedeniyle aday olarak kaldı. Sağlıklı kontrol bireyler (TA1-02 ve TA1-05) için c.598G>A varyantı homozigot yabanıl tip olarak bulundu. Ayrıca, bu varyant TA2-01 ve TA2-02 bireyleri için homozigot yabanıl tip olarak tespit edildi. Dahası, TA1-03 ve TA1-04, TA teşhisi konmuş bireyler, c.347G>A için heterozigot durumdaydı. Ancak, c.347G>A varyantı sağlıklı kontrol bireyi TA1-02'de heterozigot durumda bulunduğu için elendi.c.598G>A patojenik varyantın etkilerini araştırmak amacıyla, PPP1R32 geninin klonlandığı bir vektör içinde spesifik nükleotid değişimi (c.598G>A) yönlendirilmiş mutagenez ile başarılı bir şekilde gerçekleştirildi. Daha sonra, varyantın hücre kültüründeki etkilerini incelemek için THP1 hücre hattı, PMA kullanılarak makrofaja farklılaştırıldı. LPS (200/ng ml) ve ATP (5 mM) ile inflamazom kompleksi oluşturulmuş olup, aktif kaspaz-1 ve aktif IL1B seviyelerine immunoblotlama ile bakılmıştır.

Anahtar sözcükler: AAA, TA ,İnflamazom, Hücre Kültürü, kaspaz-1, IL1B

1. INTRODUCTION

1.1. Autoinflammatory Diseases

Autoinflammatory diseases are determined by systemic inflammation related to the innate immune system and induced by inflammasomes. These diseases are distinct from infections and are not associated with antigen-specific T cells or autoantibodies (1).

The innate immune response has undergone evolutionary development with the primary purpose of safeguarding organisms against both exogenous and endogenous threats, which may inflict harm or result in the detriment of the organism. The innate immune system aims primarily to remove the source of injury and restore tissue and homeostatic functionality. (2). The pathogenesis of autoinflammatory syndromes can be attributed to the aberrant activity of the innate immune system. As a primary defense mechanism, the innate immune system employs signaling receptors called pattern-recognition receptors (PRRs) to identify and respond to the presence of pathogens upon entry into the body. These pattern-recognition receptors are crucial in detecting danger signals and identifying and distinguishing PAMPs (pathogen-associated molecular patterns) or DAMPs (damage-associated molecular patterns). Moreover, the absence of antigen-specific T cells and autoreactive antibodies activates inflammasome complexes and causes the pathogenesis of autoinflammatory diseases (3-5). In this thesis, Takayasu Arteritis and Familial Mediterranean Fever, which are two different inflammatory diseases, are addressed.

1.2. Overview of Takayasu Arteritis

Takayasu arteritis is a disease that affects vessels such as the aorta and pulmonary arteries and is characterized by chronic inflammation. The disease mainly affects young women between the ages 15-30. The disease is caused by various non-specific symptoms such as weight loss, muscle pain, fever, and arthralgia.

The inflammation in arteries can give rise to the thickening of the blood vessel walls, which may result in severe issues such as arterial stenosis, ischemia, and developing occlusion (6).

Moreover, Cellular infiltration in aortic tissues is recognized to involve monocytes, neutrophils, and natural killer (NK) cells, along with both CD4□ (helper) and CD8□ T (cytotoxic) cells (7). Aside from cell-mediated autoimmunity, growing evidence indicates that the pathogenesis of TAK may also include antibody-mediated autoimmunity. In addition, Takayasu Arteritis has been linked to elevated serum and Fc-receptor-related immune complexes (8).

Takayasu Arteritis disease progresses in three which are Phase I (prepulseless), phase II (pulseless), and Phase III (fibrotic). Phase I identified symptoms such as mild fever, weight loss, joint pain, loss of appetite, and night sweats. Moreover, phase II is the vasculitis stage, and patients show vascular symptoms such as discomfort and pain in blood vessels. Phase III, also known as the final stage, is characterized as an occlusive, fibrotic phase in which distinctive disease features linked to occlusion arterial stenosis become evident (9).

The first recorded instance of TA in literature is ascribed to an 1830 report by Rokushu Yamamoto. In this study, he provided a detailed account of a 45-year-old male who presented with an absent radiant pulse and elevated fever. In Morgagni's study in 1861, he emphasized that a 40-year-old female showed symptoms of large vessel aneurysms and stenotic lesions. Additionally, the woman suffered from radial pulse deficiency, similar to the TA phenotype (10). To diagnose and classify Takayasu Arteritis disease, Ishikawa and the American College of Rheumatology have outlined specific diagnostic criteria (11-12). These criteria are as follows for criteria of Ishikawa (13):

- The onset of the disease should occur at 40 years of age or younger (Obligatory).
- Uptake of the mid-left subclavian artery (Major)
- Uptake of the mid-right subclavian artery (Major)

- Hypertension (Minor)
- Lesions in the pulmonary artery (Minor)
- Elevated Erythrocyte sedimentation rate (Minor)
- Lesions in the abdominal aorta (Minor)
- Lesions in the carotid artery (Minor)

For a person to be diagnosed with the disease, the individual is expected to have at least two major criteria or one major and at least three minor criteria of Ishikawa's diagnostic criteria. This is steady with a diagnosis of Takayasu Arteritis, with a specificity of 95%.

Moreover, the criteria below, on the other hand, are the criteria applied according to the American College of Rheumatology (14).

- Onset of the disease should occur at the age 40 or below.
- Advancement and deteriorated fatigue
- Discomfort in the muscle extremities
- Reduced brachial artery pulse
- Occlusion of the entire aorta and its major branches

According to the American College of Rheumatology diagnostic criteria, patients should have more than three criteria in order to be diagnosed with Takayasu arteritis. This diagnostic criterion is consistent with a specificity of 98% (14). Approximately 5% of individuals diagnosed with TA are in their childhood or adolescence. The diagnosis in most children occurs between the ages of 8 and 13. Additionally, females exhibit a higher prevalence than males at a ratio of 3:1 (15-16).

Furthermore, a recent study demonstrated that female individuals diagnosed with TA typically exhibit a higher frequency of affection in the thoracic aorta and its branches; on the other hand, in males, the involvement of the abdominal aorta and its branches is more commonly observed (17).

Hence, considering these gender-specific distinctions, it may be crucial to adopt or modify the diagnostic criteria for Takayasu Arteritis based on gender.

1.2.1. Epidemiology of Takayasu Arteritis

Although Takayasu Arteritis is prevalent globally, it is believed that the impact of the disease is considerably more significant among the Asian population (18). Takayasu arteritis exhibited the highest reported prevalence in Japan, with 40 cases per million, while in the United States, the recorded minimum frequency was 0.9 cases per million (19). Moreover, Kuwait has the highest observed incidence ratio, with 2.2 cases per million, followed by Japan, with 1-2 cases per million.

According to the research accompanied in the Aegean coasts of Turkey state that the prevalence of Takayasu Arteritis is 14.7 (20). At the same time, in the northwestern Turkey, where the population assumed was ≥16 years old, this value reaches up to 33/1,000,000 (21). Previous studies demonstrated that there is an unequal distribution of Takayasu Arteritis between sexes, with a higher susceptibility observed in women compared to men (22).

Another study suggested that the incidence of Takayasu Arteritis is six times higher in women compared to men (23).

Therefore, it might be essential to take into account both ethnicity and gender not only when examining prevalence and incidence values for TA but also when assessing the severity and progression of the condition (24).

1.2.2. Genetics of Takayasu Arteritis

Although it is recognized that the disease is most widespread in East Asia and has been thoroughly described regarding its etiology, limited information is available regarding the potential genetic factors contributing to its development, despite compelling indications (25).

The primary genetic involvement in TA is demonstrated through its connection with the human leukocyte antigen (HLA) locus. This locus encompasses six HLA genes as well as 132 protein-coding genes, the products of which play roles in regulating the immune response, antigen presentation and processing (26).

A study demonstrated that the HLA-B52 allele exhibits the most notable association within the HLA region among the Japanese population; however, various other HLA alleles, such as HLA-B39, HLA-DRB11502, and HLA-DRB10405, have also demonstrated associations with the disease in the Japanese population (26). The confirmed correlation with HLA-B*52 has been established in cases originating from Korea, India, Thailand, and Turkey, providing scientific validation across diverse populations (27). Even though the connection between the HLA locus and susceptibility to TAK has been verified, investigations into genetic components beyond HLA are still ongoing (28).

In addition, a study conducted in Japan showed that single nucleotide polymorphisms (SNPs) in the MLX gene, responsible for encoding the transcription factor MLX (Max-like protein X), have a significant and significant association with Takayasu arteritis (TAK) in Japanese patients. This SNP with rs665268 code in the *MLX* gene corresponds to a missense variant, resulting in amino acid substitution of Q139R within the DNA-binding pocket of the MLX protein.

Moreover, according to the study, the Q139R substitution promotes amendment in the structure of the MLX, which elevates the activity of the NLRP3 (NACHT, LRR, and PYD domains-containing protein 3) inflammasome and oxidative stress (29).

Additionally, another study pointed out that novel gene susceptibility loci for Takayasu Arteritis revealed crucial parts in the pathogenesis of this disease. In this study, two cohorts of individuals with Takayasu's arteritis were from Turkey and North America.

The North American cohort was composed of 134 European-descendent patients and 1047 controls. 559 patients and 489 controls were included in the Turkish cohort for this study. They identified genetic susceptibility loci associated with Takayasu arteritis, reaching genome-wide significance in the *IL6* (rs2069837) gene (30). Interleukin-6 (IL-6) belongs to a family of proinflammatory cytokines that induce the expression of several proteins associated with inflammation (31). The aberrant and persistent production of IL-6 exerts a pathological impact on chronic inflammation and autoimmunity (32) .

Another gene susceptibility loci assoiated with TA is *RPS9/LILRB3* locus (rs11666543) which is located on chromosome 19q13.4 (30). This locus contains several gene members of the leukocyte immunoglobulin-like receptor family, recognized for being expressed on antigen-presenting cells and other immune-competent cells. Moreover, these genes interact with HLA class I molecules (33). Gene polymorphisms might increase or reduce the expression of cytokines or other related molecules, leading to the development and worsening of Takayasu's Arteritis (34).

1.2.3. Immunopathogenesis of Takayasu Arteritis

While the exact mechanism behind TAK's development remains unclear, the origin of this disease probably lies in a sustained inflammatory reaction triggered by a genetically predisposed individual (35). The inflammatory activity generally affects the inner lining of the blood vessels and develops from a granulomatosis inflammation in the early phase of the disorder and, development and proliferation of smooth muscle in the arteries, fibrosis and, eventually stenosis in the large arteries are observed in the later and advanced stage of the disease (36-37). The correlated and crucial contributors in the development of Takayasu arteritis is shown in Figure 1.

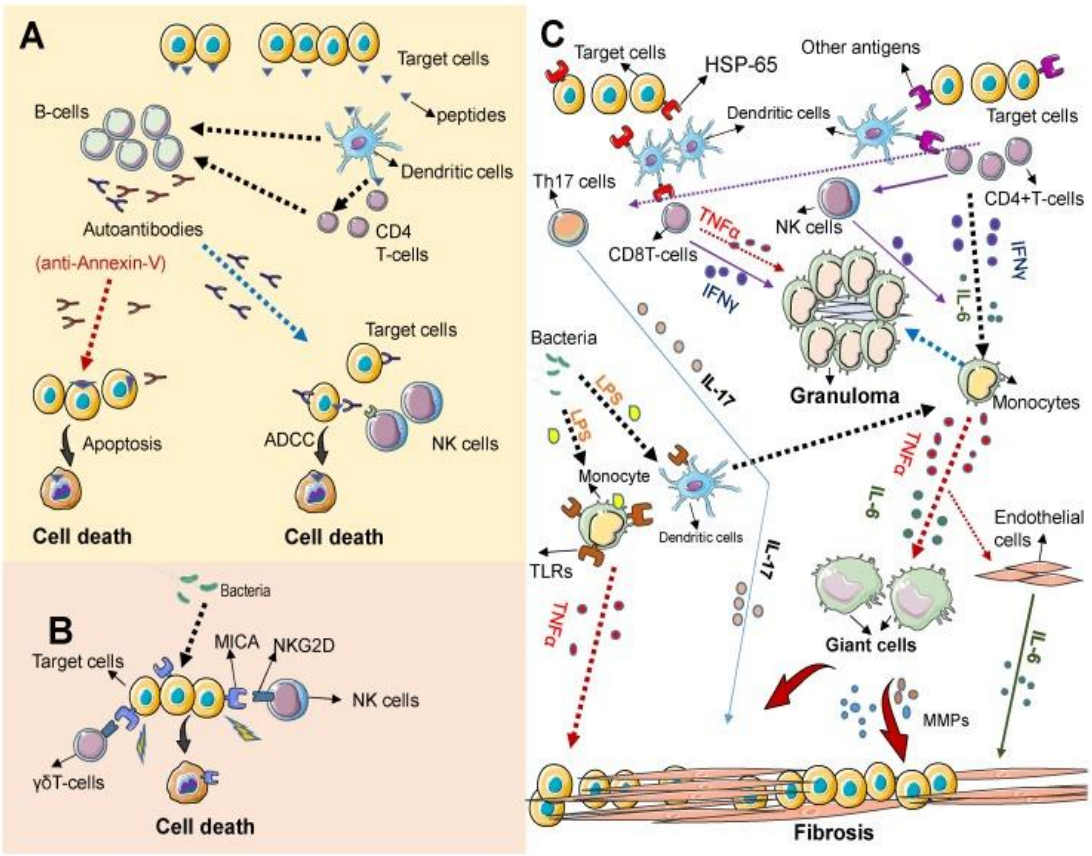

Figure 1.1: Related partners in the pathogenesis of Takayasu's Arteritis (38).

Major and intermediate-sized arteries are recognized as sites with immune privilege, employing mechanisms to restrict immune-inflammatory outputs (38).

For instance, dendritic cells localized in blood vessels hinder the entry of lymphoid cells and dampens immune reactions (39). Upon encountering an unexpected stimulus, these vascular dendritic cells undergo a process called maturation and secrete some cytokines or interleukins such as IL -23, IL-12, and IL-1β. Moreover, upon this signal, vascular T cells are activated. Hence, they migrate toward the wall of the artery (40). One possible mechanism contributing to vascular fibrosis in TA involves the initiation of inflammatory M1 macrophages and regenerative M2 macrophages (41).

For instance, studies have indicated that in the course of active inflammation in TA, the arterial wall experiences infiltration by M1 macrophages. In contrast, M2 macrophages become more prevalent in the fibrotic phase of the disease. For macrophages to promote myofibroblast proliferation and artery wall edema, macrophages must secrete growth factors such as TGF-β and PDGF (42-43).

Besides, in damaged tissues and the bloodstream, inflammatory cells that infiltrate the affected area release significant amounts of interleukin-6 (IL6) and interleukin-1 (IL1). These cytokines are believed to play a role in maintaining dysregulated immune activation by triggering the endothelial cells and commencing lymphocytic infiltration (44).

Apart from T-cells, Th17 and Th1 cells, which release interleukin-7 (IL-17) and interferon-gamma (IFN-γ), respectively, are observed to undergo substantial expansion, resulting in elevated concentrations of their corresponding cytokines (45). Hence, the pathophysiology of the disease is promoted by autoimmune-induced inflammation, vascular restructuring, and impairment in endothelial function.

1.3. Overview of Familial Mediterranean Fever

Familial Mediterranean fever (FMF) stands out as the prevailing autosomal recessive autoinflammatory disorder triggered by a monogenic mutation (46). It predominantly impacts individuals with roots in the East Mediterranean region (Arabs, Armenians, Turks), although cases have been documented globally (47).

FMF typically begins between the ages of 5 and 15, and the majority (90%) of individuals acquire the condition before reaching the age of 20. Patients typically show no symptoms between episodes, occurring from once a year to twice daily (48).

Individuals diagnosed with familial Mediterranean fever commonly experience inflammation of the peritoneum, pleura, joints, and fever. (49). Systemic AA amyloidosis, the primary contributor to illness and death, is most frequently observed in individuals with FMF (50). After the identification of AA amyloidosis, end-stage renal disease generally emerges within a five-year timeframe, and the reported survival rate for the subsequent five years stands at 50% (51).

The diagnosis of FMF is based on the Tel-Hashomer clinical criteria, which require either the presence of two or more major symptoms or the presence of one major symptom and two minor symptoms. The criteria are as follows (52):

- AA-type amyloidosis occurring in the absence of an underlying condition (major)
- Positive reaction to consistent colchicine therapy (major)
- Repetitive episodes of fever accompanied by serositis (major)
- Familial Mediterranean fever observed in a family member of the first-degree (minor)
- Repeated occurrences of fever (minor)
- Reddish skin inflammation resembling erysipelas (minor).

1.3.1. Epidemiology of Familial Mediterranean Fever

FMF stands out as the most commonly encountered monogenic autoinflammatory disorder, exhibiting a particularly elevated frequency within communities of Sephardic Jewish, Armenian, Turkish, and Arab heritage (53).

Nevertheless, there are documented cases of numerous FMF patients originating from Europe, North America, and Japan. This Figure is anticipated to rise due to substantial population migrations from regions with endemic prevalence to these areas over the past two decades (53-54).

Within the Armenian population, approximately one in seven individuals are carriers of FMF, while the rate of observed disease stands at about 1 in 500 individuals. In the Israeli Jewish community, carrier prevalence varies, ranging from one in eight people of Ashkenazi descent, one in six people of North African descent, and one in four people of Iraqi descent (55). Additionally, Turks are acknowledged for exhibiting the highest occurrence, with an estimated prevalence ranging from 1 in 150 to 1 in 1000 (56-57).

In the context of the global occurrence of FMF cases, Turkey takes the lead, with Israel and Armenia following closely, taking into account both the prevalence of the disease and the population size.

1.3.2. Genetics of Familial Mediterranean Fever

Familial Mediterranean fever (FMF) is generally regarded as an autosomal recessive disorder, and individuals affected by it carry two pathogenic mutations in the MEFV gene situated on the short arm of chromosome 16 (58-59).

MEFV gene contains 10 exons and 781 codons. Moreover, over 370 different variations have been recognized up to the present time. The number of these variations is growing due to the application of genome sequencing.

In addition, approximately 75 percent of FMF chromosomes in representative cases of Armenian, Arab, Jewish, and Turkish populations can be attributed to five significant mutations, namely E148Q, Met680Ile, Met694Val, Val726Ala, and Met694Ile (60).

Besides, M694V stands out as the most prevalent mutation among all four populations, with its occurrence ranging from 20 to 65 percent (61).

A study analyzed the most common mutations (E148Q , M680I, V726A, M694V) in a cohort of young male Turkish individuals diagnosed with FMF, and the study demonstrated that the M694V mutation was found in 80% of the FMF patients. The presence of homozygosity for the M694V mutation in the *MEFV* gene is linked to arthritis in individuals with FMF. On the other hand, other M680I, E148Q and V726A mutations were not related to specific symptoms or signs in FMF patients (62).

Another study involved a study cohort that included 33 individuals exhibiting either homozygosity or heterozygosity for E148Q, 34 with compound heterozygous E148Q mutations, and 86 patients harboring homozygosity for the M694V mutation. They pointed out that individuals with solely the E148Q mutation were identified to exhibit the highest average age at the onset of the disease and the lowest average severity score (63). Additionally, a different study stated that the E148Q variant alone is not presumedly disease-causing in children with FMF (64).

Another study demonstrated that FMF patients with the V726A or E148Q variant show a milder phenotype of the disease than other mutations (65). Hence, patients with either one or no pathogenic variant in the *MEFV* gene generally experience a less severe phenotype of the disease when compared to those with two pathogenic variants (66).

Despite the fact that the classical FMF phenotype is typically transmitted through autosomal recessive inheritance, individuals carrying heterozygous *MEFV* variants exhibit a comparable clinical manifestation to those who are homozygous for the same variants (67) and, also, FMF patients without any MEFV pathogenic variants (10-20%) imply the genetic heterogeneity of FMF (61). For instance, a study indicated that exome sequencing was performed on two different families which do not have any variants on *MEFV* gene.

They found that two different heterozygous missense variants (p.Cys72Phe and p.Arg121Gln) in *TNFRSF1A* gene in one family, and, novel,homozygous missense variant (p.Cys161Arg) on *MVK* gene in another family (90). Hence, FMF patients might carry rare variants on other genes rather than *MEFV* gene.

1.3.3. *MEFV* gene and Pyrin protein

MEFV gene is located on the short arm of human chromosome 16 at position 13.3. It contains 10 exons, producing a long transcript encoding a 781 amino acid protein (68).

This gene encodes a protein called pyrin (86 kDa), and this protein is predominantly expressed in immune cells such as monocytes, dendritic cells, neutrophils, and eosinophils, but not at remarkable levels in lymphocytes (69).

The Pyrin protein is associated with an aberrant reaction of the innate immune system and IL-1β levels during recurrent episodes of fever (70). Furthermore, pyrin is a member of cytosolic pattern recognition receptors called PRRs, which are responsible for regulating innate immune responses upon recognizing danger signals known as pathogen-danger-associated molecular patterns (PAMPs - DAMPs) (71).

Pyrin is later recognized for its interaction with the adapter protein apoptosis-related stain-like protein containing CARD (ASC), which is central to forming the inflammasome complex that triggers the caspase-1 activation. With activation and maturation of caspase-1, it cleaves pro- IL-1ß (35 kDa) to mature IL-1ß (17 kDa) and leads to the secretion of mature IL-1ß which is a pro-inflammatory cytokine (72).

1.3.4. Pyrin Inflammasome in Familial Mediterranean Fever

Pathogenic variants found in the *MEFV* gene preferentially promotes the activated state of pyrin, triggering the secretion and release of pro-inflammatory cytokines and inducing pyroptosis (73). Pyroptosis is a caspase- dependent cell death triggered by pathological stimulus and resulting in IL-1β secretion (74). For the pyrin oligomerization, certain domains such as the beta-box, alpha-helical, and coiled-coil domains are thought to be involved in the process.

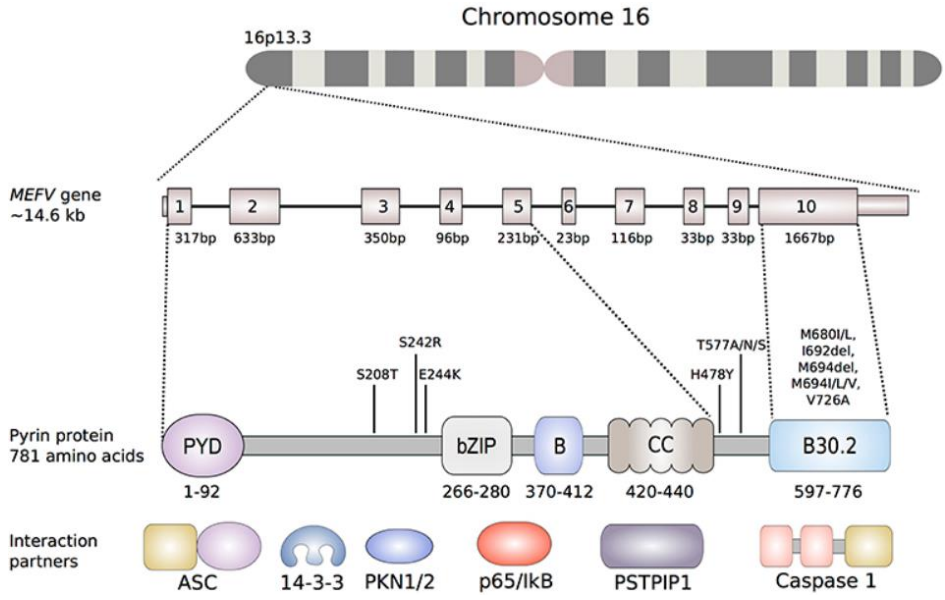

Figure 1. 2: Schematic representation image of the *MEFV* gene and pyrin protein (5).

The coiled-coil, alpha helical and the B-box domains might have a role in the pyrin oligomerization as shown in Figure 2 .

The B-box and the coiled-coil, alpha helical domains have also been shown to bind to proline-serine-threonine phosphatase-interacting protein (PSTPIP1) (5). PSTPIP1 protein has a crucial role in cytoskeleton organization. Missense mutations within *PSTPIP1* gene lead to autosomal dominant autoinflammatory syndrome identified as arthritis, pyoderma gangrenosum, and acne (PAPA) (73).

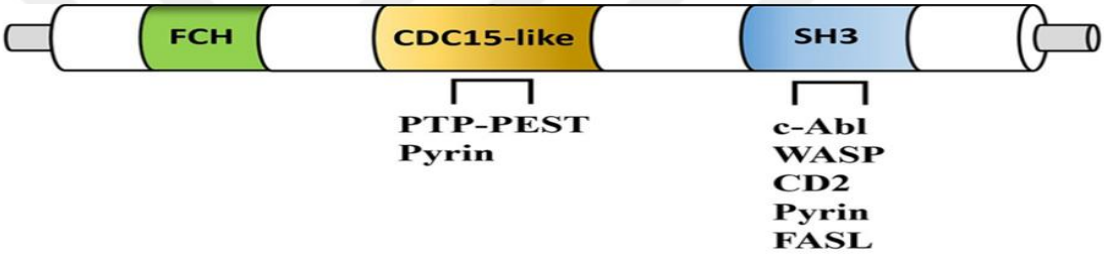

Figure 1. 3: Schematic representation of PSTPIP1 protein structure and its interacting partners (92).

PSTPIP1 gene is located on the long arm of chromosome 15 and contain 15 exons which encode a protein of 416 amino acids (75). PSTPIP1 protein is found significant levels in spleen, bone marrow and lymph node (76). It contains the Fes/CIP4 domain (FCH), CDC15-like adaptor protein (CDC15-like), and SRC Homology 3 domain.

It has an interaction with Pyrin and PTP-PEST proteins on CDC15-like domain. The PSTPIP1 protein is able to interact with c-Abl kinase, the Wiskott–Aldrich syndrome protein (WASP), CD2 and Fas ligand (FASL) on SH3 domain as shown in Figure 3 (92).

Mutations in PSTPIP1 that lead to PAPA syndrome disrupt the interaction with PEST which is rich in proline (P), glutamic acid (E), serine (S), and threonine (T))-type protein tyrosine phosphatase (PTP-PEST) (73).

PTP-PEST is cytosolic protein (120 kDa) which is predominantly expressed in spleen and thymus (77). A study pointed out that two prevalent missense variants (p.A230T and p.E250Q) linked to PAPA syndrome give rise to the phosphorylation of PSTPIP1 gene (73).

These missense pathogenic variants are located in CDC15 domain of the *PSTPIP1* gene. This domain has a crucial role for PSTPIP1 interaction with PTP-PEST. This phosphorylation result in decreased binding to PTP-PEST (79).

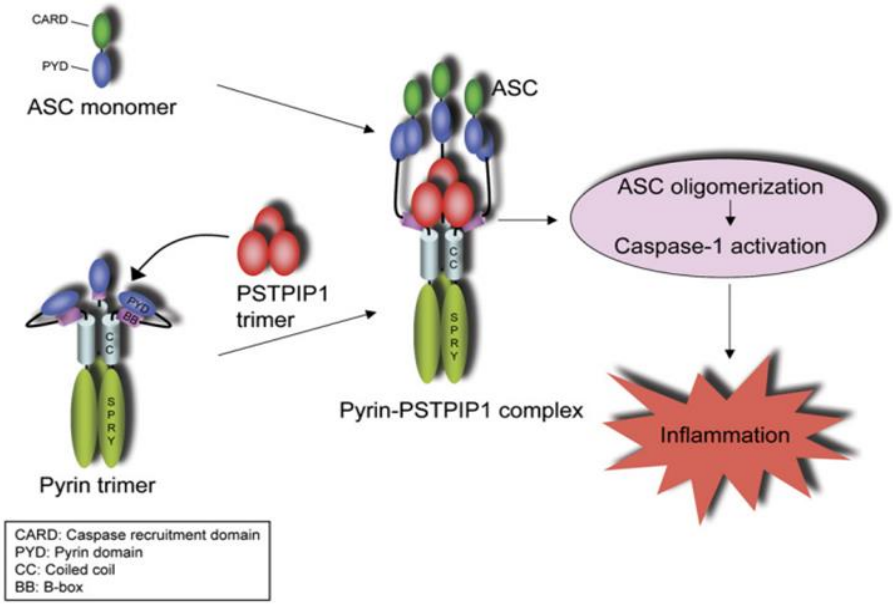

Figure 1. 4: Schematic representation of Pyrin-PSTPIP1 complex (91).

Initially, Pyrin inflammasome is in a state of inhibition. The PYD domain of ASC protein is masked by the B-box domain of pyrin protein.

When PSTPIP1 homotrimer binds to the pyrin homotrimer, the PYD domain of pyrin is unmasked. In this way, the PYD domain is now free to bind the pyrin homotrimer. The proximity of ASC monomers in close contact with the surface of the pyrin homotrimer stimulates ASC oligomerization. ASC oligomerization can induce activation of the caspase-1 (91).

Hence, this hyperphosphorylation enhances the binding affinity of PSTPIP1 to pyrin. Due to the hyperphosphorylation of PSTPIP1 triggers the pyrin inflammasome and induces caspase-1 activation and elevated levels of IL-1β production and secretion (73).

Another study demonstrated that a variant p.Arg228Cys in the *PSTPIP1* gene results in an elevated interaction between PSTPIP1 and pyrin, leading to higher levels of cleaved caspase-1 and mature IL-1β in patients exhibiting an FMF/MKD-overlapping phenotype (78). Hence, both diseases are associated with the hyperproduction of IL-1β.

Another study indicated that PSTPIP1 and pyrin proteins interact and the two proteins converge when cells are undergoing migration. The study also pointed out that Pyrin and PSTPIP1 could collaborate in activating the regulation of innate immunity (80).

These studies held importance as they established a connection between the two diseases via a shared pathway and proposed a disturbance that might be strategically addressed for therapeutic objectives.

1.4. Sequencing Technologies

Autoinflammatory disorders are caused by uncontrolled activation of the innate immune system, representing systemic inflammation in patients (81).

Diagnosing rare autoinflammatory disorders are challenging due to clinical and genetic heterogeneity (82). It took 15 years and $2.7 billion to sequence the first human genome in 2003. Progress in sequencing technologies has significantly lowered expenses, making it now possible to resequencing an entire human genome for $1000 in a single day (83).

Therefore, the development and progression in sequencing technology have enabled to identify pathogenic variants for several disorders. Hence, the many advanced sequencing technologies ensure valuable understanding into autoinflammatory diseases.

Through sequencing technologies, personalized therapy and molecular diagnostic might be provided for autoinflammatory and autoimmune diseases (84).

2. BACKGROUND AND AIM OF THE STUDY

As next-generation genome and exome sequencing techniques progress, it becomes apparent that many disorders previously categorized as 'Mendelian' diseases do not strictly conform to the single-gene inheritance model. One of the fundamental elements constituting the basis of this problem is the initial identification of disease genes through linkage and exome sequencing methods, primarily in a limited number of families.

Another significant aspect is the clinical heterogeneity present in most diseases, which not only complicates the differential diagnosis in conditions with overlapping symptoms but also emphasizes the importance of genetic diagnosis.

In this thesis, two different inflammatory diseases are addressed which are Familial Mediterranean Fever and Takayasu Arteritis.

In the first part of the thesis is to investigate the functionality of the p.R228C (NM_003978.5: c.682C>T, rs781341816) and p.A372V (NM_003978.5: c.1115C>T, rs200188483) missense variants in the *PSTPIP1* gene in in vitro cell culture models of pyrin inflammasome in multiple affected individuals from families diagnosed with AAA who do not carry pathogenic variants in the *MEFV* gene, which is the gene of the disease.

In the second part of the thesis, the aim is to investigate the potential role of the p.G200S (NM_145017.3: c.598G>A, rs148713373) missense variant in the *PPP1R32* gene which is found in multiple affected individuals from a family in the inflammasome using an in vitro cell culture model.

3. MATERIALS AND METHODS

3.1. Materials

3.1.1. Pedigree of TA1 and TA2 family

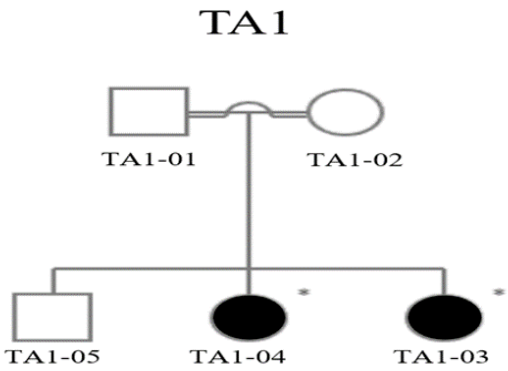

Figure 3.1. Pedigree of the family TA1. Except TA1-01,other family members (TA1-02,TA1-03,TA1-04,TA1-05 are included in this study. Dark shaded members are patients.

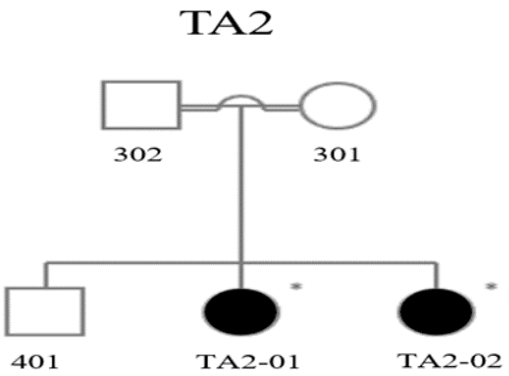

Figure 3.2. Pedigree of the family TA2. TA2-01 and TA2-02 are included in this study. Dark shaded members are patients.

3.1.2. Mammalian Expression Vectors

In this study, two different mammalian expression vectors were used. Vector maps are shown at Figure 3.3 and 3.4.

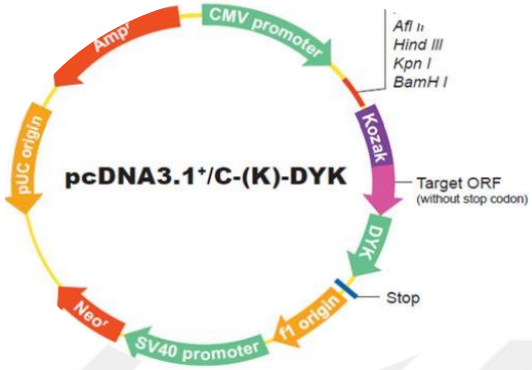

Figure 3.3. Representative image of pcDNA3.1+/C-(K)DYK vector map

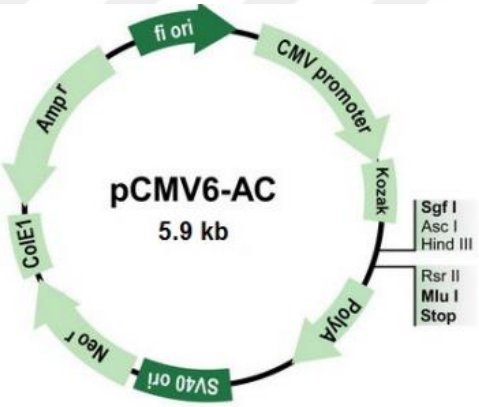

Figure 3.4. Representative image of pCMV6-AC vector map (without target ORF)

3.1.3. Buffers and other solutions

LB (Luria Bertani) Broth: 25 grams of LB broth was dissolved in 1L ddH_2O. The solution was sterilized by autoclave then stored at +4□C.

LB agar plate: 40 grams LB Agar powder was added to 1L MiliQ water. Sterilization was carried out by autoclaving. LB Agar cooled to < 50□C before addition of Ampicillin. Ampicillin was used at a final concentration of 100 µg/ml in agar plates.

Ampicillin (100mg/mL): 0.5 grams ampicillin was dissolved in 5 ml ddH_2O and was filtered through 0.22 μm PVDF filter.

10X Running Buffer: 30 grams Tris Base, 144 grams Glycine and 10 grams SDS were dissolved in ddH_2O to a final volume 1L and, kept at room temperature (RT).

10X Wet Transfer Buffer: 30.3 grams Tris Base and 144.4 grams Glycine were dissolved in ddH_2O to a final volume 1L, and, kept at room temperature (RT).

1X Wet Transfer Buffer: 100 ml of the concentrated transfer buffer (10X), 200 ml of methanol and 700 ml of ddH_2O were mixed and kept at +4□C.

10X TBS: 24.2 grams Tris Base and 80 grams NaCl were mixed in ddH_2O at 1L final volume, pH was adjusted to 7.6 by HCl and kept at room temperature (RT).

TBS-T (0.05% (v/v) Tween): 500 ml of 1X TBS and 250 μl Tween were mixed and, kept at room temperature.

5% BSA (Bovine Serum Albumin): 2.5 g BSA was weighed and dissolved in 40 ml of TBST. Placed in 4□C for 10 minutes, then, filled up the volume to 50 ml with TBST.

Cell Lysis Buffer: 50 mM Tris-HCI (pH 7.4), 1% Triton-X, 150 mM NaCI, 5 mM EDTA were mixed with ddH_2O and supplemented with 1X Protease inhibitor cocktail before use and kept on ice.

10% Ammonium Persulfate (APS) (w/v): 1 g of APS dissolved in 10 ml of ddH_2O. The solution was filtered through 0.22 μm filter and, kept at -20□C.

10% Sodium dodecyl sulfate (SDS) (w/v): 10 g SDS dissolved in 80 ml of ddH_2O in the bottle. Placed on magnetic stirrer to mix the solution and heated up the solution on the magnetic stirrer. When solution was fully dissolved, solution was completed with ddH_2O to 100 ml and, kept at room temperature.

1.5 M Tris-HCI (pH 8.8): 18.15 grams Tris base was dissolved in 80ml of ddH_2O. pH was adjusted to 8.8 using 6N HCI. The solution was completed with ddH_2O to 100 ml and, store at 4□C.

0.5 M Tris-HCI (pH 6.8): 6 grams of Tris base was dissolved in 80 ml of ddH_2O. pH was adjusted to 6.8 using 6N HCI. After pH adjustment, the solution was completed with ddH_2O to 100 ml and, kept at 4□C.

5X Laemmli Buffer: 0.125 M Tris-HCI (pH 6.8), 4% SDS, 5% B-mercaptoethanol (B-ME), 20% glycerol, 0.01% bromophenol blue solution were dissolved in 20 ml ddH_2O then stored at -20□C.

2X Laemmli loading buffer: 1 M Tris-HCI (pH 6.8), 10% SDS, 20% glycerol, 0.1% bromophenol blue solution were dissolved in 25 ml of ddH_2O, aliquoted 1.5 ml microcentrifuge tubes and, kept at -20□C. 5% B-mercaptoethanol was added freshly before use.

6X DNA loading dye: 0,009 g bromophenol blue, 1.2 ml 0.5 M EDTA (pH 8.0), 11 ml glycerol and 2.8 ml of ddH_2O were mixed, aliquoted into 1.5 ml microcentrifuge tubes and kept at -20□C.

0.5 M Ethylenediaminetetraacetic acid (EDTA) (pH 8.0): 18.61 g of EDTA were mixed in 80 ml of ddH_2O on the magnetic stirrer. The pH was adjusted with NaOH pellets to pH 8.0. After the pH adjustment, the solution was completed with ddH_2O to 100 ml. Sterilization was carried out by autoclaving.

PBST (0.1%) (v/v): 100 ml of 1X PBS and 1 ml of Tween were mixed on the magnetic stirrer and stored at room temperature.

3.1.4. Equipment

The detailed equipment list used in this thesis is given in Appendix A.

3.1.5. Chemicals

Detailed list of chemicals is given in Appendix B.

3.2. Methods

3.2.1. Genotyping for *PPP1R32* c.598G>A and c.347G>A variants

To reveal if the healthy controls and Takayasu Arteritis patients have these two variants (c.598G>A and c.347G>A in *PPP1R32* gene), Sanger sequencing (Macrogen) was performed. Before Sanger sequencing, primers were designed for each variant confirmation on *PPP1R32* gene using Primer3 Plus software, and primer quality were evaluated by using Oligoanalyzer Tool. A

dditionally, primers were checked whether they bind to another place on genome using PrimerBlast (NCBI) and UCSC In-Silico Program. Designed primers are shown at Table 1.

Table 1. Primers targeting *PPP1R32* insert

Region	Primer Sequence (5'→3')	Amplicon Size	Tm	GC%
PPP1R32 c.598G>A	F: CCTGGACTCTGGAATCCTCA R: ACATTGGCTACACCTCCTTCA	485 bp	58 □C	55 % 47.6 %
PPP1R32 c.347G>A	F: GAAGCTCCTTAGCAGAGGACA R: ATAGAGGTGGTGGGGATGGT	400 bp	60 □C	54.5 % 55 %

F: Forward Primer, R: Reverse Primer

Polymerase chain reaction (PCR) was performed for healthy controls (TA1-01,TA1-02,TA1-05) and TA patients (TA1-03,TA1-04 and TA2-01,TA2-02) by using Platinum Taq DNA Polymerase (Invitrogen, Carlsbad, California). Polymerase chain reaction (PCR) settings and components are given table 2 and 3, respectively.

Table 2. Thermal Cycling Conditions

Steps	Temperature	Time	Cycles
Initial Denaturation	94 ºC	2 min	1 cycle
Final Denaturation	94 ºC	30 sec	35 cycle
Annealing	59 ºC	30 sec	
Extension	72 ºC	30 sec	
Final Extension	72 ºC	1 min	1 cycle

Table 3. PCR Components

Components	Stock Concentration	Final Concentration
10X PCR Buffer, Minus Mg	10X	1X
dNTP Mixture	10 mM	0.2 mM
$MgCI_2$	50 mM	1.5 mM
Primer Mix	10 µM	0.2 µM
Template DNA	-	50 ng
Platinum™ Taq DNA Polymerase	5 U/µl	1 U/µl
Autoclaved, filtered ddH_2O	-	To 12.5 µl

Before Sanger Sequencing, all PCR products were examined by agarose gel electrophoresis system. To make 1% agarose gel, 0.5 g agarose and 50 ml 1X TAE buffer were mixed and microwaved for 1 min until the agarose is completely dissolved. PCR products were loaded on 1% agarose gel and run on 100V for 40 minutes. After electrophoresis, bands were visualized using ChemiDoc MP (BIORAD).

3.2.2. Preparation of Competent Cells (DH5a)

Inoculate a 5 ml overnight culture in Luria-Bertani (LB) Medium without antibiotics and allow it to grow overnight at 37□C with agitation at 250 rpm. Subsequently, inoculate 100 ml of LB medium with 1/100 volume of the overnight culture, cultivating it until reaching an OD600 of 0.5-0.6 at 37□C with agitation at 250 rpm. Transfer the cells into two sterile 50 ml centrifuge tubes and incubate them on ice for 20 minutes. Following this, centrifuge for 5 minutes at 4500 rpm and 4□C, discarding the supernatant.

Next, resuspend each pellet in 20 ml of ice-cold 100 mM CaCI2, and incubate on ice for 1 hour and 30 minutes. Centrifuge again for 5 minutes at 4500 rpm and 4□C, discarding the supernatant. Suspend each pellet in 2 ml of ice-cold 85 mM $CaCI_2$ containing 15% glycerol. Finally, pipette 100 µl into pre-cooled 1.5 ml microcentrifuge tubes and store at -80□C for future use.

3.2.3. Transformation of Plasmid DNA into E.coli by using Heat-Shock

Bacterial transformation was performed using DH5a competent cells via heat-shock method. 50 ng of circular DNA was introduced into the 50 µL of DH5a competent cells, pipetting up and down, and incubate the mixture on ice for 30 minutes. Transfer the tubes with DNA and E. coli to the heat block at 42°C for 45 seconds. Then, tubes placed to ice for 2 minutes to minimize damage to the E. coli cells. Add LB Broth (without antibiotic) to a volume of 1 ml and incubate the tubes for 1 hour at 37□C in an orbital-shaker incubator.

After incubation, centrifuge the tubes at 5000 rpm for 5 minutes, discard the supernatant, leaving 100 µL of sample. Dissolve the bacterial pellet by pipetting and spread approximately 100 µL of the resulting culture on LB plates with ampicillin. Allow the plates to grow overnight at 37□C in a bacterial incubator. After 16 hours of incubation, pick colonies for further analysis.

3.2.4. Inoculating a Bacterial Cultures

After the transformation, colonies were picked for obtaining plasmid DNA for PPP1R32 and PSTPIP1 plasmids.

In order to inoculate a bacterial culture, 100 ml LB Broth media was prepared both for PPP1R32 and PSTPIP plasmids. Afterwards, 100 µg/ml was added to the 250 ml flasks. Then, a single colony was selected from agar plates by using a sterile 200 µl pipette tips. The pipette tip was dropped into the liquid LB+ampicillin and swirled.

Then, the liquid cultures were loosely covered with sterile aluminum foil. Liquid cultures were incubated at 37□C for 12-18 hour in an orbital shaker incubator at 250 rpm (BIOSAN). After 16-hour incubation, growth was checked, which is characterized by a cloudy haze in the media.

3.2.5. Plasmid DNA Isolation

In order to study the effects of these variants on cell culture, plasmid DNA isolation was performed using Genopure Plasmid Midi Kit (Roche Diagnostics, Mannheim, Germany) according to the manufacturer's protocol.

3.2.6. Site-Directed Mutagenesis

In order to elaborate the effects of variants, site-directed mutagenesis was performed to mutate signified nucleotides of a DNA sequence within a plasmid vector.

To create a specific mutation in a DNA sequence, mutagenic primers were designed for each variant (c.598G>A for *PPP1R32* and c.682C>T, c.1115C>T for *PSTPIP1*). Mutagenic primers were designed by using PrimerX software. Designed primers are given at table 4.

All primers have a phosphate modification at their 5' ends to facilitate a downstream intramolecular ligation reaction.

Table 4. Mutagenic Primers for *PPP1R32* and *PSTPIP1* insert

Gene and region	Primer Sequence (5'→3')	Tm (□C)	GC%
PPP1R32 c.598G>A	F: GCAGAAGAAATCGATCAGCGCAAAGGAGGGGAG R: CTCCCCTCCTTTGCGTGATCGATTTCTTCTGC	72 □C	55%
PSTPIP1 c. 682C>T	F: GCTGACCATTCTCTGCAACGCCCTGTG R: CACAGGGCGTTGCAGAGAATGGTCAGC	70 □C	59 %
PSTPIP1 c.1115C>T	F: GCTATCTGGGTTCTGCACTGTATAATCGTA R:GCTCATCTGGGTTCTGCACTGTATAATCGTAGA	71 □C	49%

F: Forward Primer, R: Reverse Primer

Site-directed mutagenesis was carried out using Q5 High-Fidelity DNA Polymerase (NEB, Massachusetts, USA).

All PCR products were examined by agarose gel electrophoresis system. PCR products were loaded on 1% agarose gel and run on 95 V for 40 minutes. After electrophoresis, bands were visualized using ChemiDoc MP (BIORAD).

3.2.7. DpnI Digestion

After site-directed mutagenesis, all PCR products were treated with Dpn1 digestion because Dpn1 (NEB, Massachusetts, USA) enzyme cleaves plasmids that have methylated sites.

This process selects for the mutated plasmids which are unmethylated by eliminating any remaining template plasmid DNA that was not mutated during the site-directed mutagenesis. The reaction was carried out using T100 Thermal Cycler (BIORAD). After the Dpn1 digestion, products were checked by agarose gel electrophoresis system. Products were loaded on 0.8% agarose gel and run 95V for 45 minutes. After the electrophoresis, bands were visualized by busing ChemiDoc Mp Imaging System (BIORAD). Incubation settings and components for digestion are shown at table 5 and Table 6, respectively.

Table 5. Thermal Cycling Condition of DpnI Digestion

Step	Temperature	Time
Digestion	37 ºC	1 hour
Heat Inactivation	80 ºC	20 min

Table 6. Components of Dpn1 Digestion

Components	50 µl RXN	Final Concentration
Restriction Enzyme (DpnI)	1 µl	10 units
DNA		-
rCutSmart Buffer	5 µl	10 X
Nuclease free water	To 50 µl	

3.2.8 DNA Purification from Agarose Gel

After gel electrophoresis, the agarose gel was placed in E-Gel® Safe Imager™ Real-time Transilluminator (Invitrogen, Carlsbad, California). DNA fragment was taken from the agarose gel using a razor blade and transferred into a microcentrifuge tube.

DNA purification was performed using commercial kits. (Nucleospin Gel and PCR Clean Up Kit , Macherey-Nagel , Germany) according to the manufacturer's protocol.

3.2.9. Colony PCR

After DNA purification from agarose gel, bacterial transformation was performed and, growing colonies were randomly selected to check if they have taken the plasmid DNA with colony PCR.

Colony PCR was carried out using Platinum Taq DNA Polymerase (Invitrogen). Genetic insert -specific primers were designed for each clone. Primers and thermal cycling conditions are given at Table 7 and 8.

Table 7. Primers for Colony PCR

Gene and region	Sequence(5'→3')	Tm (ºC)	GC (%)	Amplicon Size
PPP1R32	F: GGAAGGTCCATTTCGACACC R: GTTAAGGCTGAACCCTGTGG	59 ºC 59 ºC	55 % 55 %	1414 bp
PSTPIP1	F: TTTCCTCCCCTCAGAAGCTC R: CGCACTCCTTTATTCCCTGG	59.4 ºC 59.4 ºC	55 % 55 %	1450 bp

F:Forward Primer, R:Reverse Primer

Table 8. Thermal Cycler Conditions for Colony PCR

Steps	Temperature	Time	Cycle
Initial Denaturation	94ºC	2 min	1
Final Denaturation	94ºC	30 sec	34
Annealing	56ºC	30 sec	
Extension	72ºC	1 min	
Final Extension	72ºC	2 min	1
Hold	4ºC	∞	1

After Colony PCR, all PCR products were analyzed via agarose gel electrophoresis system. PCR products were loaded on 0.8% agarose gel and run at 95V, 40 min.

After the electrophoresis, the bands were analyzed by ChemiDoc MP Imaging System (BIORAD).

Then, these products were sent for Sanger Sequencing (Macrogen) to verify whether the mutations have created or not.

3.2.10. THP-1 Cell Line

In order to research effect of the variants on cell culture and inflammasome experiments, THP-1 cell line was used. THP-1 is a human acute leukemia monocyte cell line and has been extensively employed to investigate immune responses, encompassing not only the monocyte state but also the macrophage-like state of cells.

3.2.10.1. Thawing Procedure for THP-1 Cell Line

The THP-1 cell line is thawed in a water bath set at 37□C. Cells diluted with 7 ml of complete RPMI medium followed by centrifugation at a force of 280 x g for 5 minutes to remove dimethyl sulfoxide (DMSO), a cryoprotective agent. After centrifugation, the cellular pellet from this process is carefully resuspended in 10 ml of complete RPMI growth medium. The resuspended cellular material is then transferred to a T-25 culture flask, facilitating the continuation of the cell culture procedure.

Finally, the cells are incubated in an incubator with optimal conditions set specifically for 37□C and 5% CO_2.

3.2.10.2. Preparation of Growth Medium and Subculture of THP-1 Cell Line

RPMI-1640 with L-glutamine and sodium bicarbonate (Sigma-Aldrich) is used for this cell line as a growth medium. Additionally, 10% Heat Inactivated Fetal Bovine Serum (FBS-) (Biowest), 1 mM L-Glutamine (Gibco), 1X Penicillin- Streptomycin (P/S) (Sigma-Aldrich),10 mM HEPES (Euroclone) were used to make complete RPMI-1640 Medium.

The cell culture was established by centrifugation cell suspension at 280 x g for 5 minutes. Then, old medium was discarded and resuspended the cell pellet at a density of 2-5 x 100,000 cells/ml in fresh complete RPMI-1640 medium containing 10% FBS.

Cell culture was incubated in sterile cell culture incubator (37□C ,5% CO2). Subculturing was performed every 2 to 3 days.

3.2.11. PMA Treatment

Before starting the in vitro cell culture experiments, the THP-1 cells were treated with 400 ng/ml Phorbol 12-myristate 13-acetate (PMA) (TOCRIS). THP-1 cell line is commonly utilized model for human monocytes and macrophages. This is due to the fact that, after differentiation induced by PMA, THP-1 cells develop a macrophage-like phenotype that closely resembles primary human macrophages in various aspects. 5 mg PMA was dissolved in 250 µL DMSO (BioShop) to make 20 mg/ml PMA Stock Solution.

In order to use in experiments, 20 mg/ml PMA was diluted into 1 mg/ml using DMSO. For cell culture experiments, $1x10^6$ THP-1 was seeded into each well of 12 well plate. Afterwards, 400 ng/ml PMA was added per well of a 12 well plate (TPP, Switzerland).

After 4 hours, cell culture medium was removed from plate and fresh complete RPMI-1640 medium was added each well. Then, cells were rested overnight. After resting, cells were examined in EVOS M5000 Imaging System (Thermo Scientific) to see the monocyte to macrophage differentiation.

3.2.12. Transfection of Differentiated THP-1 Cell Line

To investigate the effects of the variants in THP-1 cell line, the cells were transfected with PSTPIP1 and PPP1R32 wild type and mutant vectors.

Transfections enable the temporary expression of a gene of interest in a specific cell line, proving beneficial for conducting short-term studies on protein function. This study used LipoFectMax™ 3000 Transfection Reagent (ABP Biosciences) for transfection.

This transfection reagent is a lipid-based transfection reagent designed to create a complex with DNA or RNA, facilitating the translocation of this complex into various adherent and suspension cell lines. This reagent exhibits exceptional transfection efficiency and enhances cell viability, proving particularly effective for a diverse range of challenging-to-transfect and commonly utilized cells.

After resting the cells for 1 day, the old medium was discarded and, fresh growth medium without antibiotics (Pen/Strep) was added to each well.

When cells are transfected, growth medium with antibiotic may cause cell death and make difficult for cells to take up foreign DNA. That's why growth medium without Pen/Strep was used in transfection experiments. For each transfection manufacturer protocol was followed. Finally, the cells were incubated at 37 37°C in a CO_2 incubator for 24 hours before checking for protein expression.

3.2.13. Inflammasome Stimulation with LPS+ATP Treatment

To create an induced-inflammasome model *in vitro*, the cells were treated with certain concentration of Lipopolysaccharide (LPS) (Invitrogen) and Adenosine triphosphate (ATP) (ChemCruz), respectively.

For LPS treatment, 500 µL fresh RPMI 1640 medium was added to each well of 12 well plate. For the LPS+ATP condition, the cells were treated with 200 ng/ml (LPS) Lipopolysaccharide for 3 hours. For this purpose, 2 µL of LPS was added to the LPS+ATP wells only, not the no-treatment (NT) wells.

After 3 hours LPS incubation, the cells were treated with 5 mM ATP for 1 hour in the LPS+ATP condition. For this purpose, 5 µL of ATP was added into the LPS+ATP wells.

3.2.14. Methanol-Chloroform Precipitation from Cell Culture Supernatant

Inflammasome activation involves the conversion of pro-caspase-1 and pro-IL-1β into their functional forms (cleaved caspase-1 and mature IL1ß) through cleavage. To detect cleaved caspase-1 and mature IL1ß in the supernatant, it is recommended to concentrate the sample through methanol-chloroform precipitation. All samples (NT, LPS+ATP) were precipitated via this method.

Following the LPS+ATP treatments, the 1 volume (500 µL) supernatant was collected into a 1.5 ml microcentrifuge tube. To this, ¼ volume (125 µL) of reagent-grade chloroform (MERCK) and an additional volume of reagent-grade methanol (500 µL) (MERCK) are added. After the addition, the sample undergoes vigorous vortexing for 30 seconds to ensure homogeneity.

The homogenized sample is then centrifugated at 13,800 x g for 5 minutes at room temperature. Post-centrifugation, the tubes are carefully removed, revealing three distinct phases: the upper methanol phase, a protein layer in the middle, and the lower chloroform phase.

With precision, the methanol phase is aspirated off without disturbing the central protein layer. Another volume of methanol (500 µL) is added, followed by a repeated centrifugation step at 13,800 xg for 5 minutes at room temperature. A visible white protein pellet is expected in all samples upon removal from the centrifuge.

To conclude the sample preparation, methanol is aspirated off without causing damage to the protein pellet. The remaining pellets are then air-dried for 5 minutes at 55□C.

Before Western blot analysis, the dried pellets undergo boiling in 40 µL of 2x Laemmli buffer for 5 minutes at 95□C. These methodical steps ensure the proper extraction and preparation of protein samples for subsequent Western blot analysis.

3.2.15. Protein Isolation from Cultured THP-1 Cells

Protein isolation was performed from adhered cells by manually.

In the initial step, 100 µL of cold cell lysis buffer is added to each sample found in the 12 well plate. Then, the wells are scraped using a sterile pipette tip to ensure the resuspension of adhered cells. The resuspended cells are then transferred into a 1.5 ml microcentrifuge tube, followed by a 15-minute incubation on ice with intermittent vortexing at 5-minute intervals.

Following the incubation, the sample centrifugated at 13,500 rpm at 4□C for 15 minutes. After that, the supernatant is transferred into a new tube and stored at -80□C for further analysis.

3.2.16. Measurement of protein samples with Bicinchoninic acid (BCA) Assay

The protein concentration of samples was measured by Bicinchoninic acid (BCA) (Pierce™ BCA Protein Assay Kit, ThermoScientific) Assay. The protein measurement was performed according to the manufacturer's protocol.

3.2.17. Protein expression analyses from supernatants and cultured THP-1 cells

After the methanol-chloroform precipitation of cell culture supernatants, cleaved caspase-1 and mature IL1ß levels were analyzed by western blotting. IL1ß (1:500; SantaCruz Biotehcnology, Dallas, USA) and caspase-1 (1:500, Cambridge, UK) primary antibodies and anti-mouse (1:2000, Cell Signaling Technology, Danvers, USA) and anti-rabbit (1:2000, Cell Signaling Technology, Danvers, USA) secondary antibodies were used in western blotting experiments. PSTPIP1, PPP1R32 and GAPDH protein levels were analyzed in the protein samples isolated from cell lysate.

PSTPIP1 (1:1000, SantaCruz Biotechnology, Dallas, USA) , GAPDH (1:1000, Cell Signaling Technology, Danvers, USA) and PPP1R32 (1:5000, ABConal, Woburn, USA) primary antibodies and anti-rabbit (1:3000, Cell Signaling Technology, Danvers, USA) and anti-mouse (1:3000, Cell Signaling Technology, Danvers, USA) secondary antibodies were used in western blotting experiments. For western blotting experiments, SDS-PAGE gels were prepared as 15%-10% (gradient) for resolving gel and 4% for stacking gel for cleaved Caspase-1 and mature IL1ß proteins manually as shown in table 9.

Table 9. SDS-PAGE Gel Preparation for WB Experiments

Component	Volume		
	15% separation gel	**10% separation gel**	**4% stacking gel**
ddH_2O	1.77 ml	1.9 ml	2.5 ml
1.5 M Tris-HCI (pH 8.8/ pH 6.8)	1.25 ml	1 ml	1 ml
40% Acrylamide	1.87 ml	1 ml	400 µl
10% SDS	50 µl	40 µl	40 µl
10% APS	50 µl	40 µl	40 µl
Temed	5 µl	4 µl	4 µl

SDS-PAGE gels were prepared as 12% for resolving gel and 4% for stacking gel for PSTPIP1, PPP1R32 and GAPDH proteins manually as given in table 10.

The justification for the preparation of a gradient gel (15%-10%) targeting cleaved caspase-1 and IL-1ß lies in the efficient resolution of distinct bands associated with cleaved caspase-1 (10-12 kDa) and IL-1ß (17 kDa).

Table 10. SDS-Gel Preparation for WB Experiments

Component	Volume	
	12 % separation gel	4% stacking gel
ddH_2O	2.6 ml	2.5 ml
1.5 M Tris-HCI (pH 8.8/ pH 6.8)	1.25 ml	1 ml
40% Acrylamide	1.25 ml	400 µl
10% SDS	50 µl	40 µl
10% APS	50 µl	40 µl
Temed	5 µl	4 µl

30 µL of precipitated supernatant mixed with 2x Laemmli buffer, ensuring an appropriate volume of protein samples isolated from cell lysates, total 20 µg of protein. Subsequently, incubate the samples at 95□C for 5 minutes, followed by placing them on ice for 30 seconds to prepare them for analysis.

5 µL of prestained protein ladder (ThermoScientific) was loaded into the first wells of each gel. Run the SDS-page at a constant voltage of 95 V for the initial 20 minutes and then set for 115 V.

When the running process was completed, transfer the gels to a 0.2 µm PVDF membrane using wet transfer system. Transfer was conducted at 100V for 30 minutes at room temperature, with the membrane submerged in ice. Following the transfer, block the membrane with 5% BSA at room temperature on a shaker for 1 hour.

After the blocking step, incubate specific portions of the membrane with the appropriate primary antibodies, diluted in 2.5% BSA-TBS-Tween (0.05%), for 30 minutes at room temperature and then overnight at 4□C. Wash the membranes three times for 10 minutes each with 1X TBS-T (Tris-buffered saline-Tween).

Proceed to incubate the membranes with the corresponding secondary antibodies at room temperature for 1 hour. Subsequently, wash the membranes again with 1X TBS-T three times for 10 minutes each. Finally, visualize the bands using the ECL kit (ThermoScientific) via the Image Lab Software (BIORAD). These steps comprise a comprehensive protocol for gel electrophoresis, membrane transfer, and immunoblotting analysis.

3.2.18. Statistical Analyses

For the analysis of Western Blot densities, Image Lab software was used. For all proteins, volume intensities were excluded from the software to Excel program and interest of protein/gapdh (as an internal control) volume intensity ratios were calculated.

4. RESULTS

4.1. Genotyping for *PPP1R32* gene variants with sequence specific PCR

PCR primers which were designed to amplify specific regions of candidate variants (c.347G>A and c.598G>A) in *PPP1R32* genes were optimized. Their bands were observed by agarose gel electrophoresis at 400 bp and 485 bp, respectively. After PCR, products were prepared for sanger sequencing to confirm the variants in TA patients and healthy controls. Agarose gel results were given in Figure 4.1.

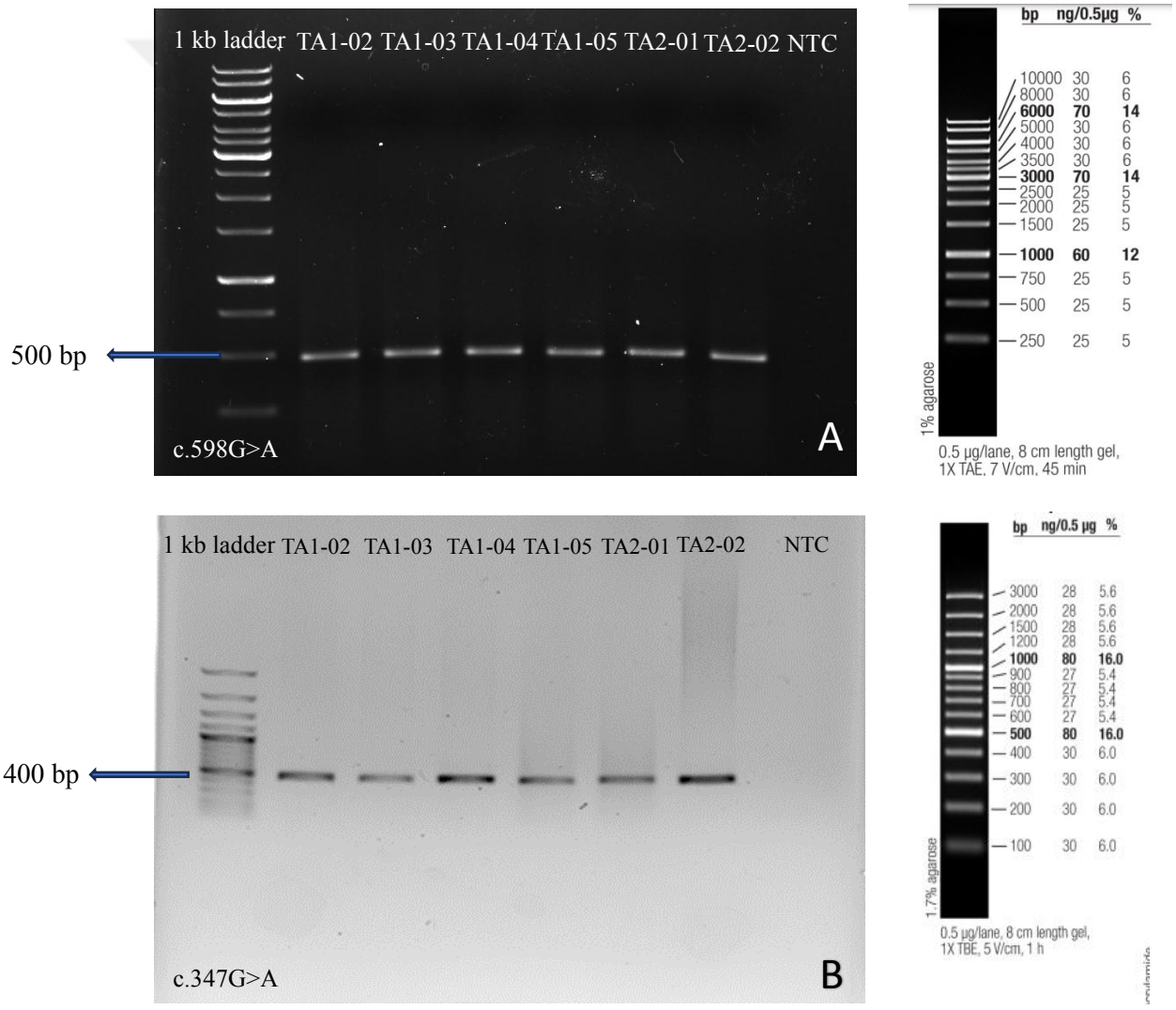

Figure 4.1. (A-B) Gel electrophoresis results images of amplified regions in TA1-03, TA1-04, TA1-05 and TA2-01, TA2-02 individuals. NTC: Negative Control.

4.1.2. Results of Sanger Chromatogram Analysis for *PPP1R32* Gene Variants

In consequence of Sanger Sequencing, c.598G>A variant was remained as candidate because of presenting as heterozygous status at individual TA1-03 and TA1-04 which are diagnosed with Takayasu Arteritis. For healthy controls (TA1-02 and TA1-05), were homozygous wild-type for c.598G>A variant. Additionally, this variant was homozygous wild-type for individual TA2-01 and TA2-02.

Moreover, TA1-03 and TA1-04 diagnosed with TA was heterozygous status for c.347G>A. However, c.347G>A variant was eliminated because of presenting as heterozygous status at individual TA1-02 who is healthy control. As a result of the sanger sequencing results, c.598G>A variant in *PPP1R32* gene was considered for further analysis. Sanger sequencing results were analyzed by using Chromas 2.6.6 software.

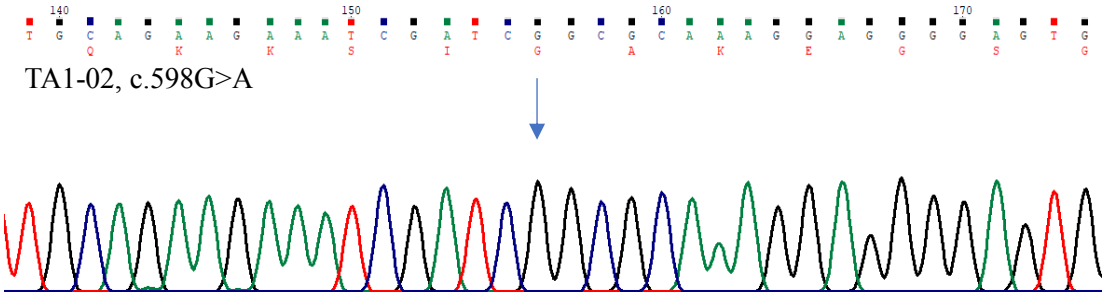

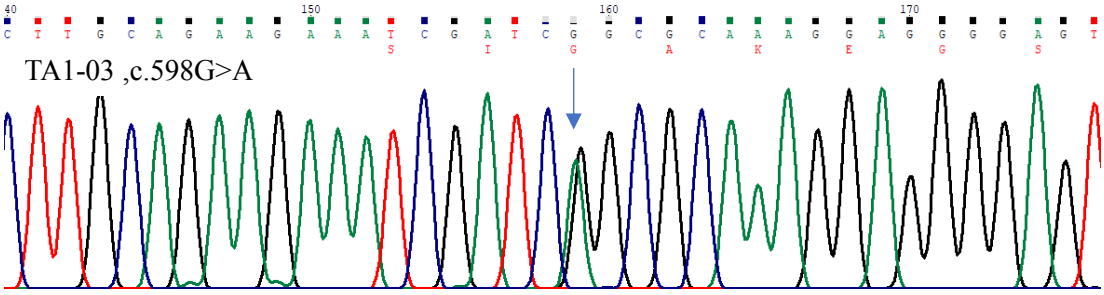

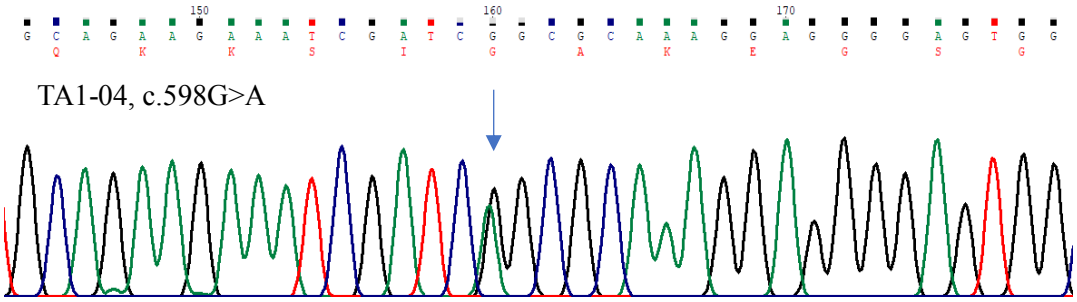

TA1-04, c.598G>A

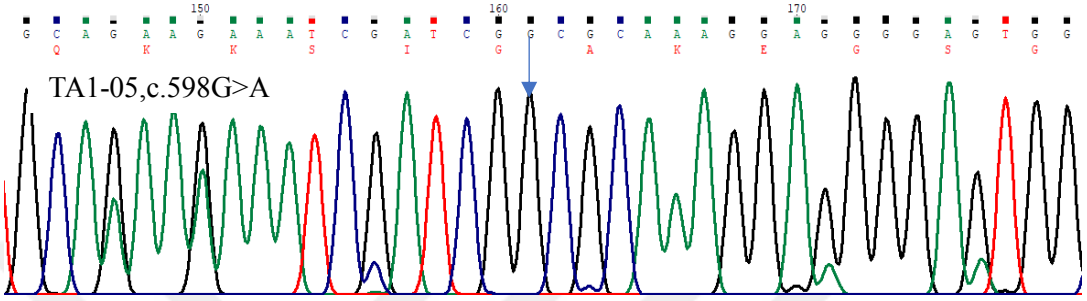

TA1-05,c.598G>A

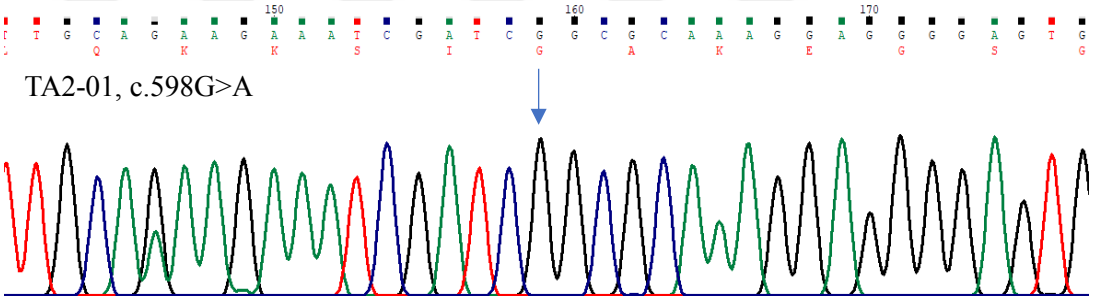

TA2-01, c.598G>A

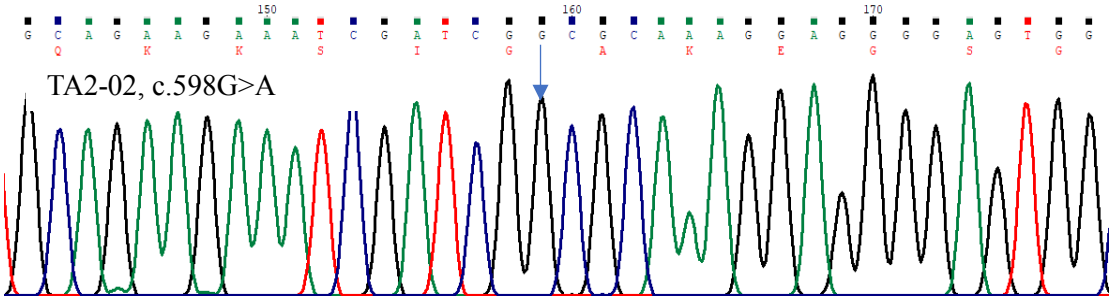

TA2-02, c.598G>A

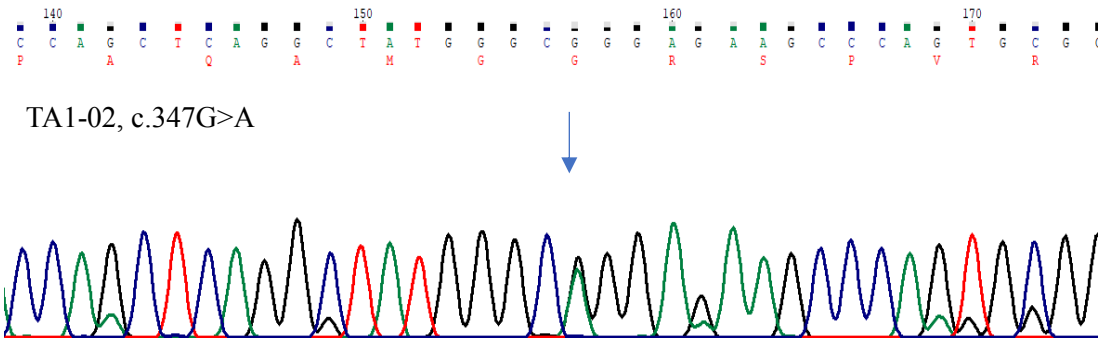

TA1-02, c.347G>A

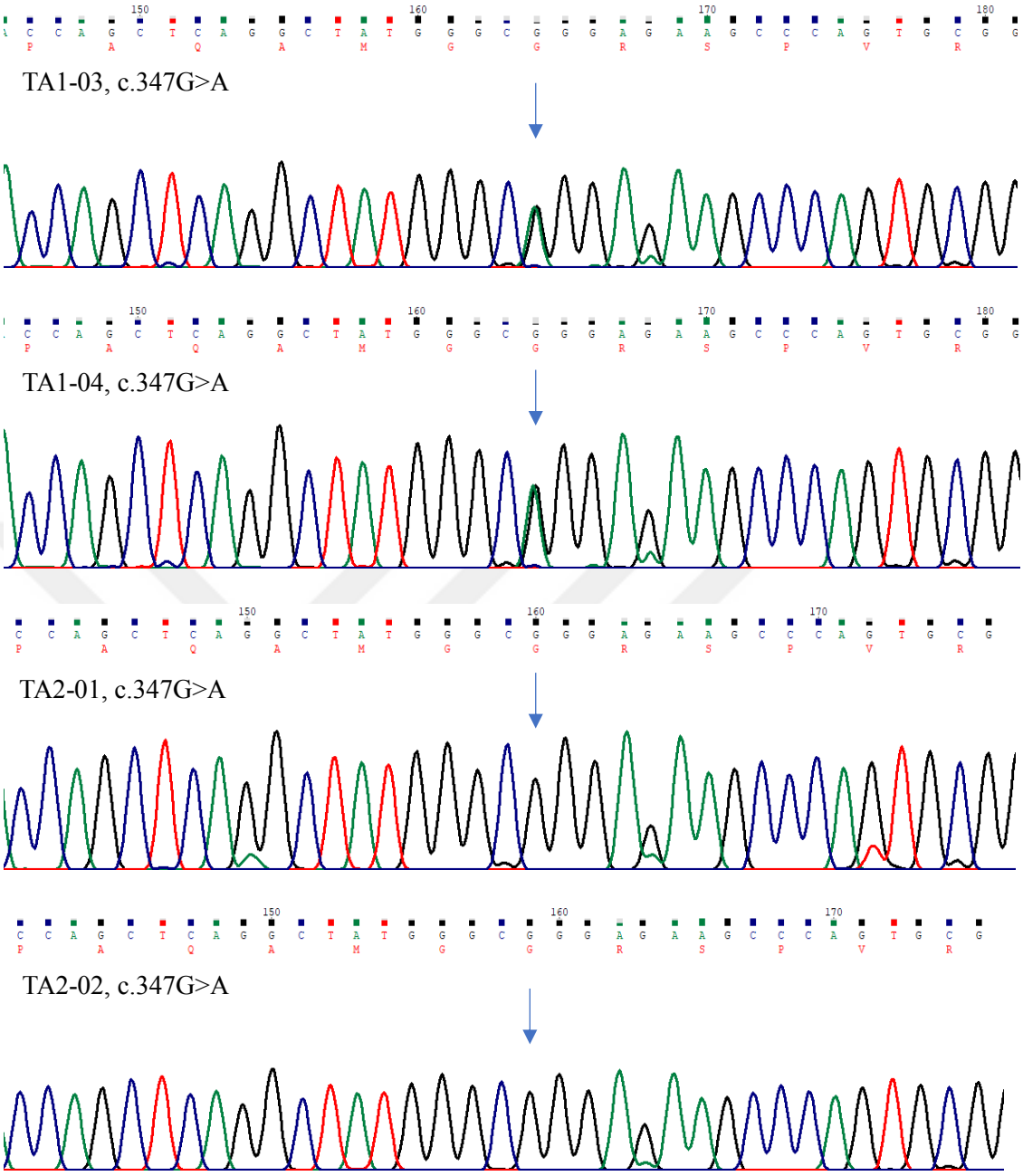

Figure 4.2. Sanger chromatogram results for c.598G>A and c.347G>A variants in TA1 and TA2 families. c.598G>A variant was heterozygous status for TA1-03 and TA1-04. It was homozygous wild-type for TA1-02 and TA1-05. C.347G>A variant was homozygous wild-type for TA2-01 and TA2-02. This variant was homozygous wild-type status for TA2-01 and TA2-02. Variant region was shown with blue arrow.

4.1.3. Site-Directed Mutagenesis Results for *PPP1R32* c.598G>A

Site-directed mutagenesis was performed employing sequence-specific mutagenic primers to alter the G nucleotide to an A nucleotide for the *PPP1R32* gene cloned into a pcDNA3.1+/C-(K)DYK vector. The plasmid vector is approximately 6.7 kb. In order to amplify the entire vector, Q5 High-Fidelity DNA Polymerase was used in site-directed mutagenesis experiments. Annealing temperature of the primers were specified according to NEB Tm Calculator version 1.16.5. Gradient PCR was utilized to find the optimized annealing temperature. All annealing temperature was successfully amplified the entire vector as shown in Figure 4.3.

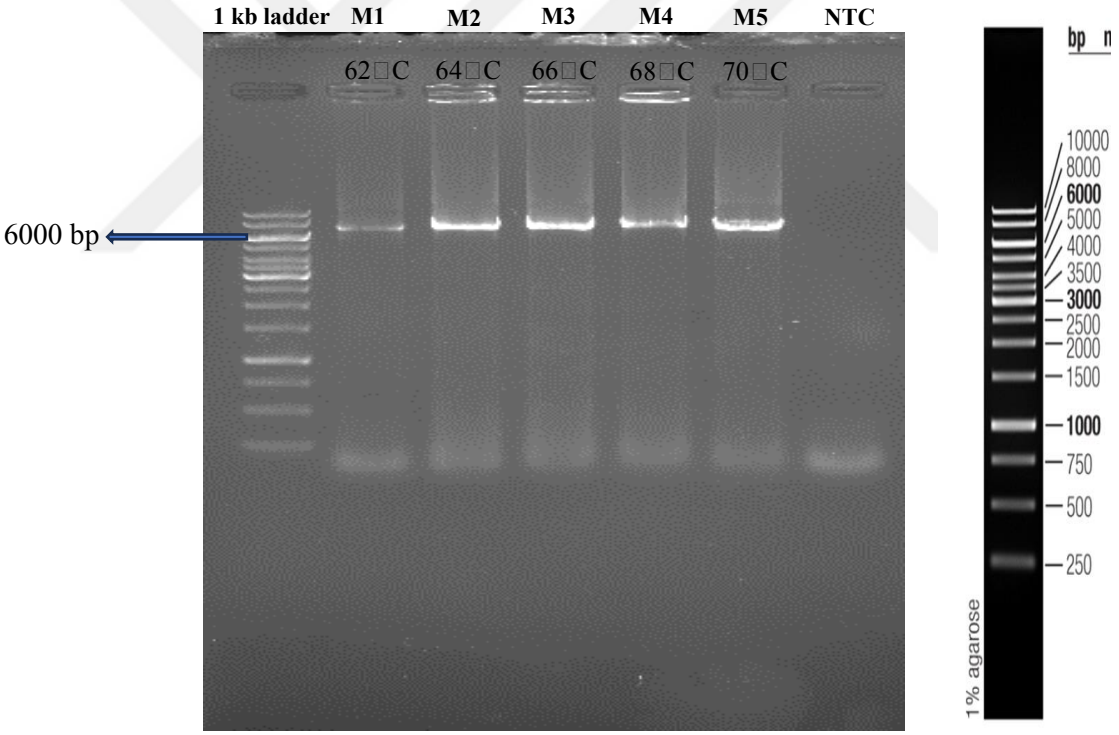

Figure 4.3. Detection of the plasmid from site-directed mutagenesis by agarose gel electrophoresis. Lanes: 1- 1 kb DNA ladder, 2-M1 (62□C), 3-M2 (64□C), 4-M3 (66□C), 5-M4 (68□C), 6- M5 (70□C) 7- NTC. M corresponds to 'mutant'.

4.1.4. DpnI Digestion Results for PCR-Based Clones

Following site-directed mutagenesis, plasmids serving as DNA templates in PCR need to undergo digestion by the restriction enzyme DpnI prior to bacterial transformation. DpnI does not cleave unmethylated products, such as PCR products; however, it exhibits high specificity for methylated DNA, such as plasmids amplified in DH5α E. colicompetentcells.

DpnI facilitated the thorough removal of plasmid templates from site-directed mutagenesis reactions (as shown in Figure 4.4), ensuring the successful elimination of undesired background colonies in subsequent cloning applications.

Following DpnI digestion, wild-type and mutated plasmid DNA were transformed into DH5α E. coli competent cells and isolated plasmid DNA from growing colonies.

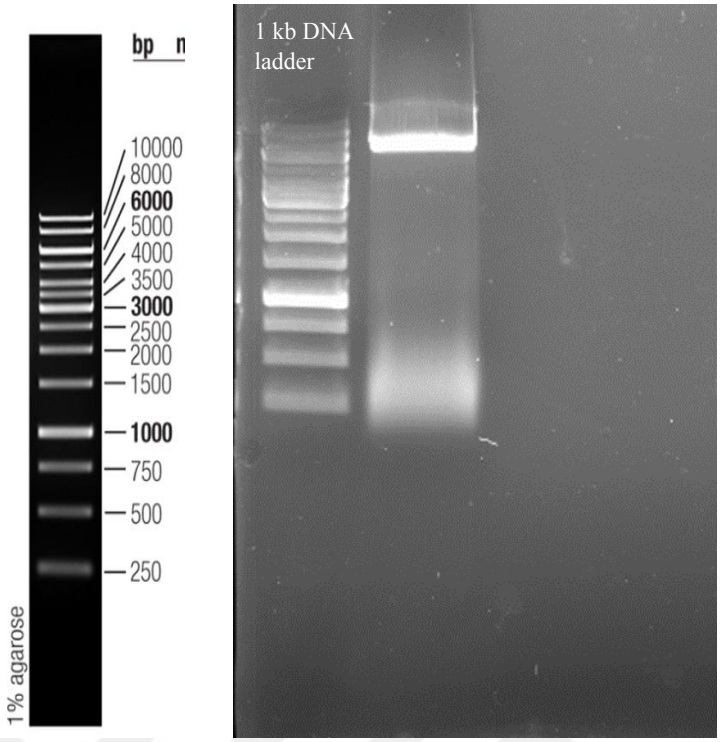

Figure 4.4. Agarose gel electrophoresis result of Dpn1 digestion. Lanes: 1- 1 kb DNA ladder, 3- Undigested PCR product after Dpn1 treatment.

4.1.5. Colony PCR Results for Wild Type and Mutated Clones

Following plasmid DNA isolation from the colonies, colony PCR was performed using insert-specific primers as shown in Table 7. Four PCR reaction was carried out for wild type clone (*PPP1R32*- WT) and mutant clone (*PPP1R32*- c.598G>A). Afterwards, 1% agarose gel electrophoresis was done whether these clones are positive or not. The results indicate that chosen colonies are the ones containing the plasmid vector as shown in Figure 4.5.

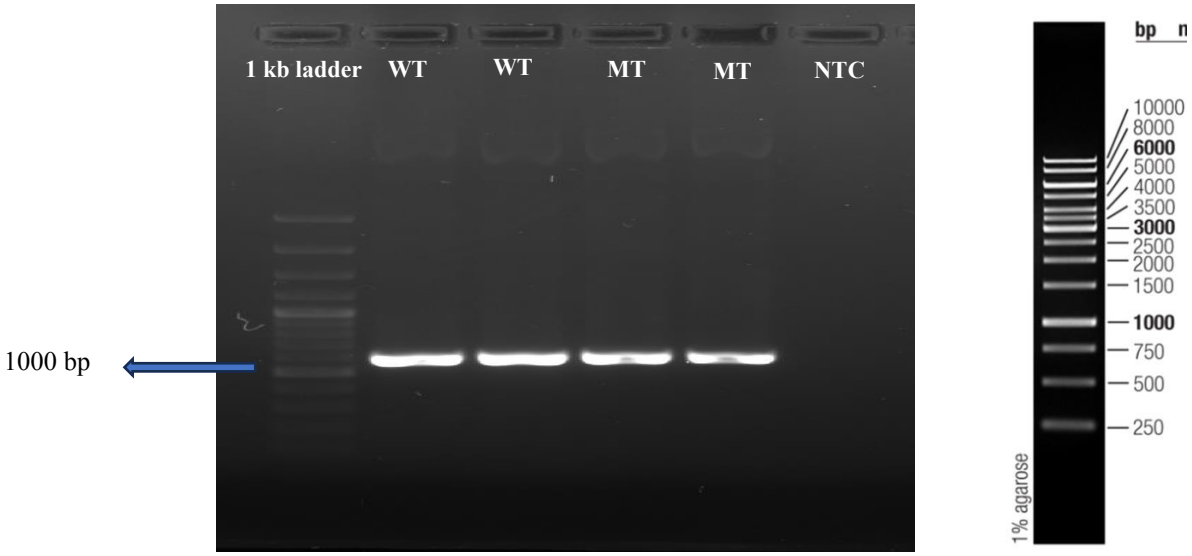

Figure 4.5. Agarose gel electrophoresis of Colony PCR Results for PPP1R32 in the pcDNA3.1+/C-(K)DYK. Lanes: 1- 1 kb DNA ladder, 2-5 colony PCR results from bacterial clones grown on LB agar after transformation , 6- NTC. WT: Wild-Type, MT: Mutant.

4.1.6. Sanger chromatogram results for Wild-Type and Mutant Clone for pcDNA3.1+/C-(K)DYK vector

Following colony PCR, products were sent to sanger sequencing (Macrogen) in order to verify the mutated nucleotide on pcDNA3.1+/C-(K)DYK vector.

The resulting chromatogram results demonstrate that G>A substitution was occurred successfully as homozygous state in mutant clone as shown in Figure 4.5.

c.598G>A [p.Gly200Ser]

A

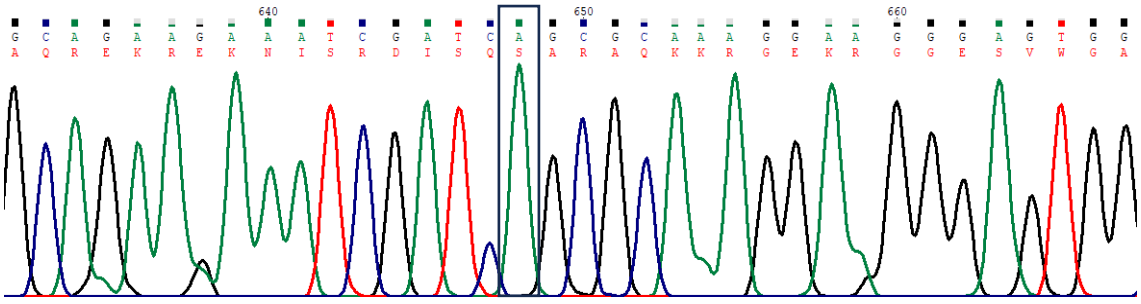

Wild-Type

B

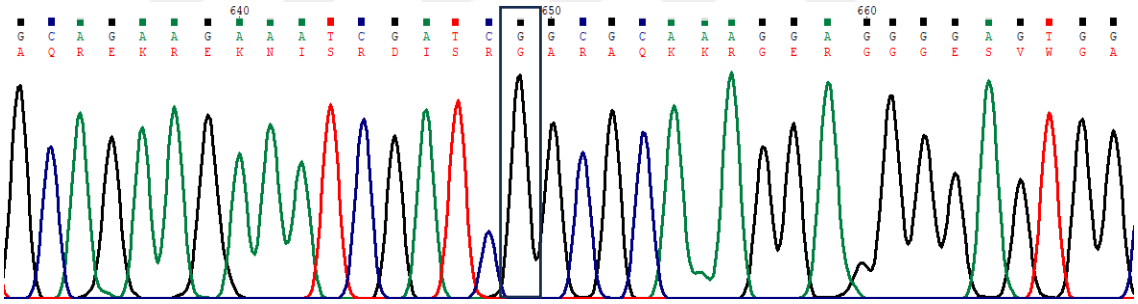

Figure 4.6. Results of sanger sequencing electropherogram for (B) wild-type and (A) mutant clone. The mutation was confirmed via sequencing the forward strand. The relevant nucleotides are highlighted within rectangle.

4.1.7. Protein Expressions in Inflammation-Induced and Uninduced Conditions

To investigate the functionality of rare missense variant (p.G200S) in the *PPP1R32* gene within the pyrin inflammasome, an inflammasome model was established in cultured and differentiated THP1 cells. Thus, to create an inflammasome model in cell culture, THP-1 cells were stimulated by Lipopolysaccharide (LPS) (200 ng/ml) for 3 hours then, Adenosine triphosphate (ATP) (5 mM) for extra 1 hour in sterile incubator (37□C, 5% CO_2). After the treatments, supernatants were collected and precipitated (methanol-chloroform) for mature IL1ß and cleaved caspase-1 expression by western blotting. For each lane,30 µl of precipitated supernatant was loaded.

Due to the poor quality of the blot results, protein quantification could not be performed. But, active IL1ß (17 kDa) is seen PPP1R32 WT and PPP1R32 G200S samples compared to No Transfection sample in LPS+ATP condition. In addition, cleaved caspase-1 (10 kDa) is also observed in uninduced conditions. The underlying cause of the issue may be that the cells have been transfected with plasmid DNA using a lipid-based method (LipoFectMAX 3000). In other words, the cells take up foreign DNA from the outside. This situation may lead to cellular stress, which could induce one of the inflammasome pathways.

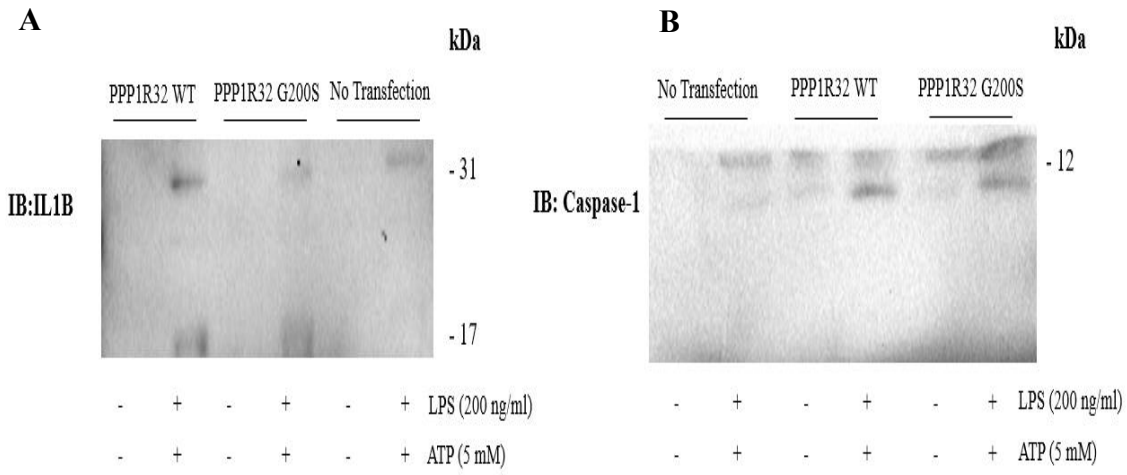

Figure 4.7. Active caspase-1 and IL1ß expression in inflammation-induced and uninduced conditions. A) Pro- IL1ß p.31 form and mature IL1ß p.17 form in supernatants of cultured THP-1 cells of samples. B) Mature caspase-1 p.10 form in supernatants of cultured THP-1 cells of samples.

4.2. Site-directed mutagenesis results for *PSTPIP1* c.682C>T and c.1115C>T

Site-directed mutagenesis was performed employing sequence-specific mutagenic primers to alter the C nucleotide to an T nucleotide for the *PSTPIP1* gene cloned into pCMV6-AC vector. In order to amplify the entire vector, Q5 High-Fidelity DNA Polymerase was used in site-directed mutagenesis experiments. Annealing temperature of the primers were defined according to NEB Tm Calculator version 1.16.5.

Gradient PCR was performed to find the optimized annealing temperature. Four PCR reactions were set up for c.682C>T whereas six reactions were set up for c.1115C>T. All annealing temperature was successfully amplified the entire vector, as shown in Figure 4.8 and Figure 4.9.

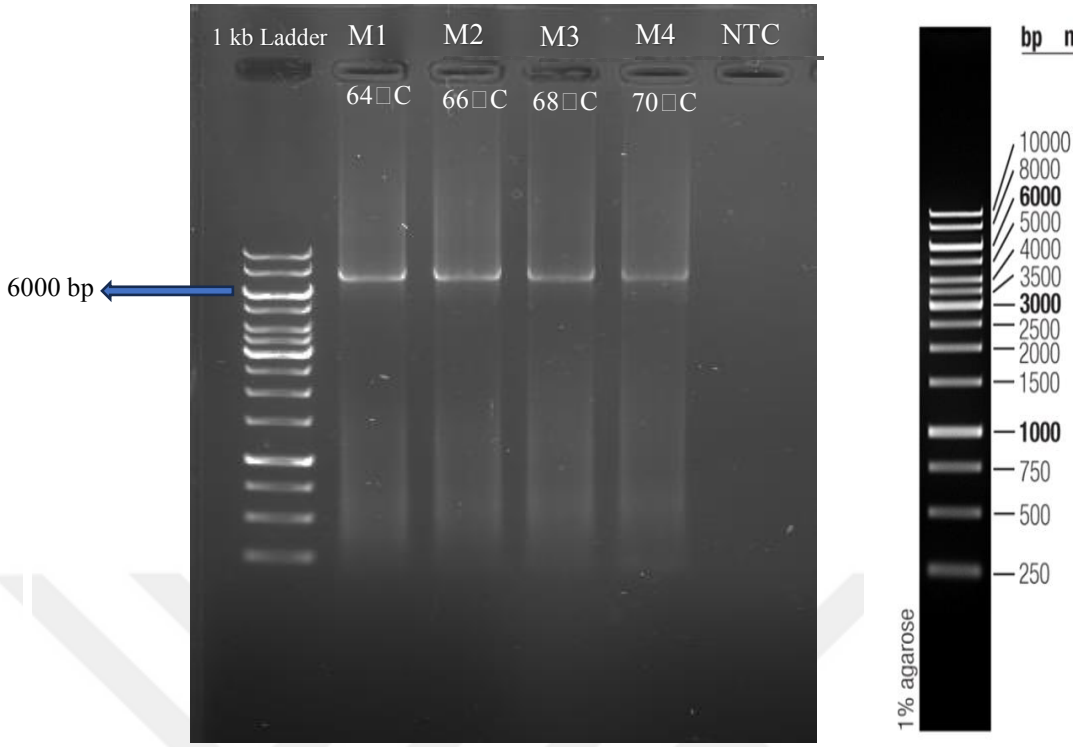

Figure 4.8. Visualization of the site-directed mutagenesis PCR products (c.682C>T) using 0.8% agarose gel electrophoresis; 100V, 45 min. Lanes:1-1 kb DNA Ladder, 2-M1 (64□C), 3-M2 (66□C), 4-M3 (68□C), 5-M4 (70□C), 6-NTC.

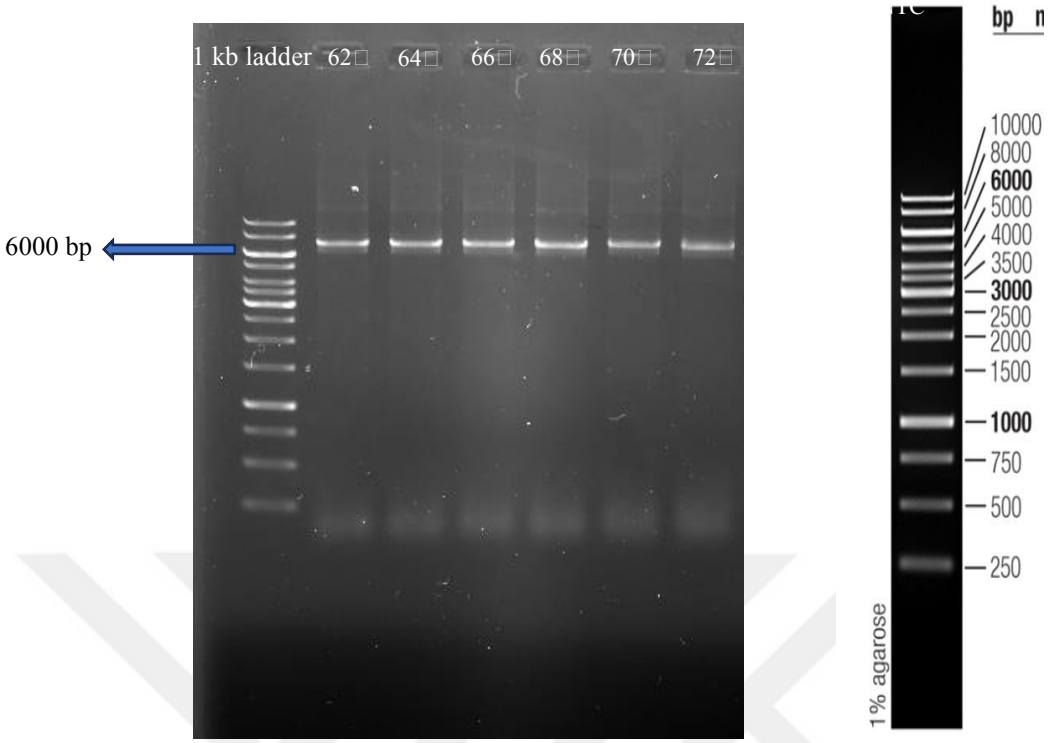

Figure 4.9. Agarose gel electrophoresis of site-directed mutagenesis PCR products (c.1115C>T). Lanes: 1- 1 kb DNA Ladder, 2- M1 (62□C), 3-M2 (64□C), 4- M3 (66□C), 5- M4 (68□C), 6- M5 (70□C), 7-M6 (72□C), 8-NTC.

4.2.1. Dpn1 Digestion Results for PCR-based Clones

After performing site-directed mutagenesis, plasmids used as DNA templates in PCR should be subjected to digestion by the restriction enzyme DpnI before undergoing bacterial transformation.

DpnI does not cut unmethylated products, like PCR products, but it demonstrates a strong affinity for methylated DNA, such as plasmids amplified in DH5α E. coli competentcells.

DpnI facilitated the thorough removal of plasmid templates from site-directed mutagenesis reactions (as shown in Figures 4.8 and 4.9), ensuring the successful elimination of undesired background colonies in subsequent cloning applications.

Following DpnI digestion, wild-type (WT) and mutated (MT) plasmid DNA were transformed into DH5α E. coli competent cells by heat shock. Plasmid DNA was isolated from growing colonies.

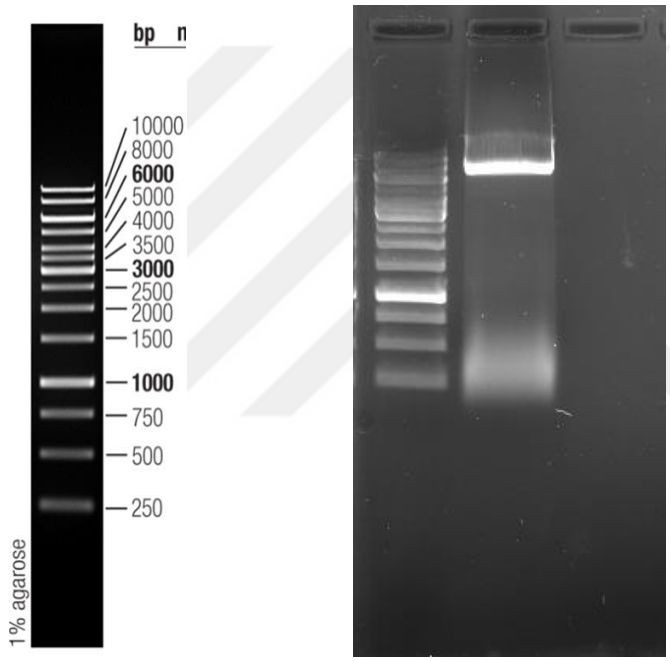

Figure 4.10. Agarose gel electrophoresis of Dpn1 digestion of plasmid (c.682C>T). Lanes 1: 1 kb DNA ladder, 2- PCR product after Dpn1 digestion (37□C for 1 hour).

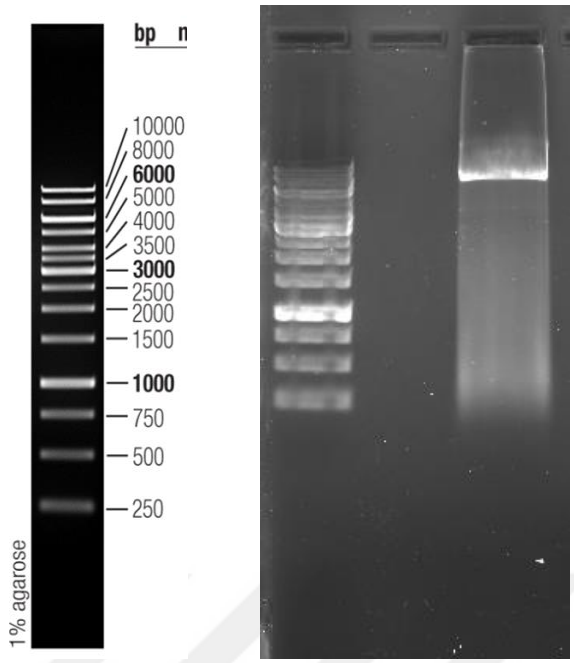

Figure 4.11. Agarose gel electrophoresis of Dpn1 digestion of plasmid (c.1115C>T). Lanes 1: 1 kb DNA ladder, 2- PCR product after Dpn1 digestion (37□C for 1 hour).

4.2.2. Colony PCR Results

Following plasmid DNA isolation from the colonies, colony PCR was performed using insert-specific primers, as shown in Table 7. Three PCR reactions were carried out for wild-type clones (PSTPIP1- WT) and mutant clones (*PSTPIP1*- c.682C>T and c.1115C>T). Afterwards, whether these clones are positive or not, 1% agarose gel electrophoresis was performed. The results indicate that the chosen colonies contain the gene insert, as shown in Figure 4.12.

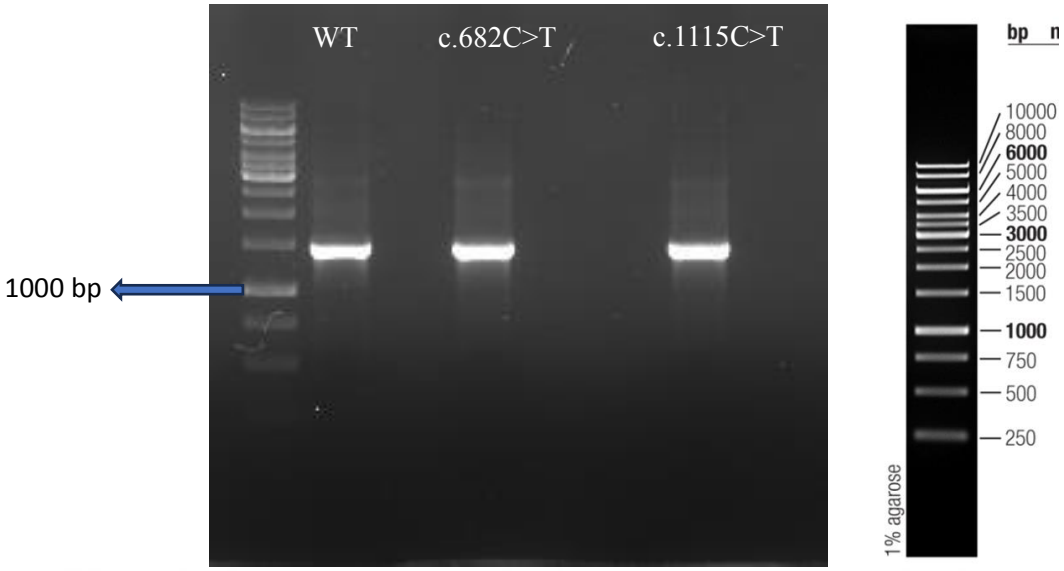

Figure 4.12. Agarose gel electrophoresis of Colony PCR Results for PSTPIP1 in the pCMV6-AC vector. Lanes: 1- 1 kb DNA ladder, 2-4-7 colony PCR results from bacterial clones grown on LB agar after transformation, 8- NTC. WT: Wild-Type, MT: Mutant, NTC: Negative Control.

4.2.3. Sanger chromatogram results for Wild-Type and Mutant Clones for pCMV6-AC vector

Following colony PCR, products were sent to Sanger sequencing (Macrogen) to verify the mutated nucleotide on the pCMV6-AC vector. The chromatogram results show that C>T substitution occurred successfully as a homozygous state for both mutant clones, as shown in Figures 4.13 and 4.14.

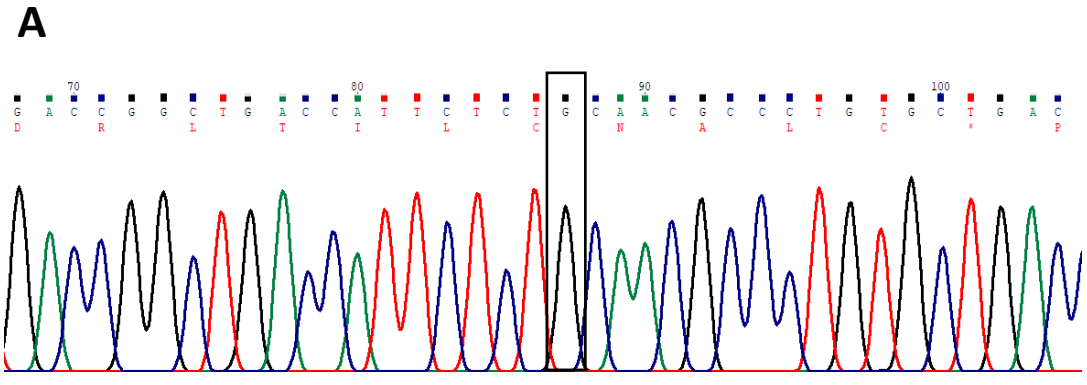

Figure 4.13. A) Results of Sanger sequencing electropherogram for c.682C>T. The mutation was confirmed via sequencing the forward strand. The relevant nucleotide is highlighted within the rectangle.

B

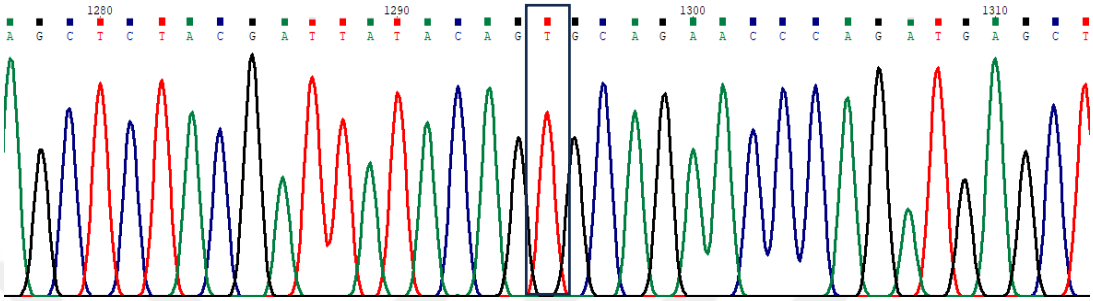

Figure 4.14. B) Results of Sanger sequencing electropherogram for c.1115C>T. The mutation was confirmed via sequencing the forward strand. The relevant nucleotide is highlighted within rectangle.

4.2.4. Protein Expressions in Inflammation-Induced and Uninduced Conditions

To investigate the functionality of rare missense variants (p.A372V and p.R228C) in the *PSTPIP1* gene within the pyrin inflammasome, an inflammasome model was established in cultured and differentiated THP1 cells. Thus, to create an inflammasome model in cell culture, THP-1 cells were stimulated by Lipopolysaccharide (LPS) (200 ng/ml) for 3 hours then, Adenosine triphosphate (ATP) (5 mM) for extra 1 hour in sterile incubator (37□C, 5% CO_2). After the treatments, supernatants were collected and precipitated (methanol-chloroform) for mature IL1ß and cleaved caspase-1 expression by western blotting. Due to the poor quality of western immunoblotting results, quantification was not performed. But, active IL1B (17 kDa) is seen in PSTPIP1 WT, PSTPIP1 A372V and PSTPIP1 R228C samples compared to No-Transfection sample in LPS+ATP condition.

In addition, cleaved caspase-1 (10 kDa) is also observed in uninduced conditions. This issue may be due to the transfection of the wild-type and mutant plasmid DNA into the THP-1 cells. Foreign nucleic acid is introduced into THP-1 cells, and this may induce cellular stress, which might cause inflammasome activation by different mechanisms.

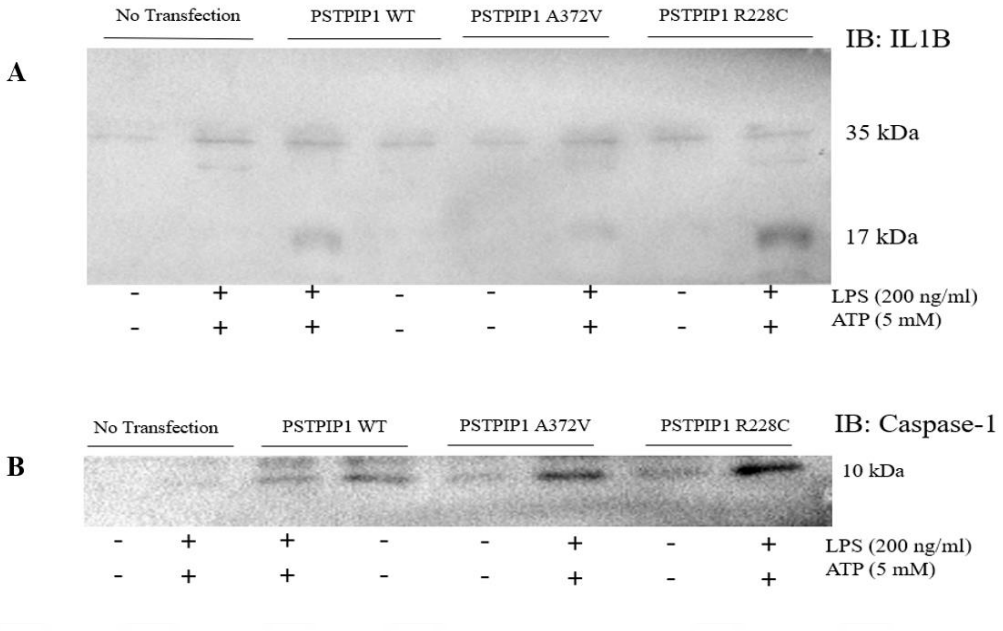

Figure 4.15. Active caspase-1 and IL1ß expression in inflammation-induced and uninduced conditions. A) Pro- IL1ß p.31 form and mature IL1ß p.17 form in supernatants of cultured THP-1 cells of samples. B) Mature caspase-1 p.10 form in supernatants of cultured THP-1 cells of samples. NT: No Transfection.

5. DISCUSSION AND CONCLUSION

The genes associated with autoinflammatory diseases have been predominantly identified since the late 1990s, often through a limited number of familial cases. The widespread adoption of next-generation sequencing technologies in routine clinical practice has accelerated the identification of new autoinflammatory diseases and genes. On the other hand, advancements in this field have blurred the known boundaries between monogenic and multifactorial forms of these syndromes and between autoinflammatory and autoimmune conditions.

Familial Mediterranean Fever disease has been associated with five missense and pathogenic variations (V726A, E148Q, M680I, M694V, M694I) found in the *MEFV* gene. However, despite being characterized as a disease with autosomal recessive inheritance, approximately 25% of patients with Familial Mediterranean Fever carry only one pathogenic variation in the *MEFV* gene, and around 10-20% of patients with FMF are observed not to have any pathogenic variant in *MEFV* (62). Hence, the presence of Familial Mediterranean Fever patients who do not carry *MEFV* pathogenic variations suggests that the etiopathogenesis of the disease may be more complex (61). In a study, it has been demonstrated that a group of MEFV-negative Familial Mediterranean Fever patients carry genetic mutations, and these different variants may lead to similar and the same phenotype (85).

In another study, a family member with MEFV-negative FMF was found to have a pathogenic variant (p.A372V and p.R228C) in the *PSTPIP1* gene, which is another inflammatory gene, and it was observed that this variant could lead to a similar phenotype (79).

In autoinflammatory diseases, problems occurring in the functions of proteins that constitute inflammasomes constitute the fundamental cause at the molecular level.

The immune system activates inflammatory pathways by engaging pattern recognition receptors in response to pathogen-associated molecular patterns (PAMP) and endogenous signals from damaged cells (86). The pyrin protein produced by the *MEFV* gene constitutes a part of the NLRP3 inflammasome complex. The NLRP3 inflammasome complex is defined as an intracellular organelle necessary for producing IL-1β (87). Pyrin plays a crucial role in the NLRP3 inflammasome complex, and a mutation in this protein results in heightened inflammation by triggering elevated production of IL-1β through the activation of caspase-1 (88).

One part of this thesis aims to investigate whether the specified *PSTPIP1* variants (p.A372V and p.R228C) in the cell culture model of the pyrin inflammasome increase inflammation or not. According to the first results, caspase-1 level is 2.6-fold higher in the PSTPIP1 p.R228C sample compared to the PSTPIP1 wild-type sample in inflammasome condition. Furthermore, the active caspase-1 level is 1.84 higher in the PSTPIP1 p.A372V sample compared to the PSTPIP1 wild-type sample in inflammasome induced condition (Figure 4.15). The PSTPIP1 protein contains an F-BAR domain located in N-terminal , the PEST motif, and the SH3 domain in C-terminal (89). The p.R228C variant is found on the F-BAR domain of PSTPIP1 protein (79). The F-Bar domain is crucial to form the functional trimeric complex with pyrin. Hence, the p.R228C variant may lead to a structural change in the PSTPIP1 protein and induce pyrin inflammasome activation. With inflammasome activation, pro-caspase-1 is cleaved into active-caspase-1, which cleaves pro-IL1B into its mature form IL1B.

In the second part of the thesis, the aim is to investigate the potential role of the p.G200S (NM_145017.3: c.598G>A, rs148713373) missense variant in the *PPP1R32* gene which is found in multiple affected individuals (diagnosed with Takayasu Arteritis) from a family in the inflammasome using an in vitro cell culture model.

Takayasu Arteritis is a rare inflammatory disease marked by inflammation of the blood vessels, this condition has the potential to impede blood circulation and harm crucial tissues and organs (40). This thesis examines two consanguineous families exhibiting multiple affected individuals within the same generation. The first TA family has a healthy mother, father, and brother, while two sisters are affected.

The second TA family shares similarities with the first, with two out of three children affected. First, gene and variant filtration was performed according to the exome data of the two families. The filtration was done according to minor allele frequency (MAF<0.01), variant effect prediction software (CADD, PolyPhen,Mutation Taster), and also the impact of the variant. Based on the variant filtration, c.598G>A and c.347G>A missense variants found on *PPP1R32* gene was selected to study. Afterwards, Sanger sequencing (Macrogen) was performed for the variants in order to study further.

According to the sequencing results, c.598G>A variant was remained as candidate because of presenting as heterozygous status at individual TA1-03 and TA1-04 which are diagnosed with Takayasu Arteritis. For healthy controls (TA1-02 and TA1-05), were homozygous wild-type for c.598G>A variant. Additionally, this variant was homozygous wild-type for individual TA2-01 and TA2-02. Moreover, TA1-03 and TA1-04 diagnosed with TA was heterozygous status for c.347G>A. However, c.347G>A variant was eliminated because of presenting as heterozygous status at individual TA1-02 who is healthy control. As a result of the sanger sequencing results, c.598G>A variant in *PPP1R32* gene was considered for further analysis.

Afterwards, a plasmid containing the DNA insert encoding the PPP1R32 protein was purchased, and site-directed mutagenesis was performed. Through site-directed mutagenesis method, the G nucleotide at position 598 was successfully substituted to an A nucleotide in a homozygous status.

In mutagenesis experiments, Q5 High-Fidelity DNA Polymerase was used instead of Taq DNA Polymerase. These types of DNA polymerases have correction capabilities that minimize errors during DNA replication, ensuring accurate amplification of the target sequence. Additionally, these types of polymerases ensure the accurate implementation of desired mutations while preserving the integrity of the target DNA sequence.

Finally, high-fidelity DNA polymerases are of significant importance in mutagenesis due to their ability to amplify much longer DNA fragments more effectively than a standard Taq polymerase. After mutagenesis experiments, PCR was performed from both wild-type and mutant plasmid DNA to confirm the substitution in the target region, followed by Sanger sequencing. According to the Sanger chromatogram results, no changes were observed in the wild-type plasmid DNA, whereas the desired nucleotide alteration was successfully achieved in the mutant plasmid DNA at the intended position.

Furthermore, chromatogram results were thoroughly examined to determine if there were any other changes in the DNA sequence during mutagenesis. Upon examination, only one nucleotide alteration was identified, and it was observed that this amino acid change still encoded the same protein.

Following the mutagenesis experiments, transfections of wild-type and mutant plasmid DNA into THP-1 cells were performed using a lipid-based method.

Due to the difficulty in transfecting THP-1 cells, a lipid-based chemical (Lipofectamine) was used. Prior to Lipofectamine-based trials, transfections were conducted using calcium phosphate.

However, the transfection efficiency was found to be very low (data not shown). According to the literature, electroporation is the most effective method for transfecting THP-1 cells, with a transfection efficiency of 60%.

Next, in order to understand whether this variant in the *PPP1R32* gene plays a role in inflammasome activation, an inflammation cell culture model was established, and later, Western blot analysis was performed to assess the levels of cleaved caspase-1 and mature IL1B (inflammasome markers). Based on the first western blot results, cleaved caspase-1 level is 1.4-fold higher *PPP1R32* p.G200S sample compared to *PPP1R32* wild type sample in inflammasome induced condition.

One of the limitations of this study is that we could not perform CRISPR/Cas9 gene editing system to remove the original sequence of PSTPIP1 and PPP1R32. In other words, we were unable to integrate the sequences containing the c.682C>T and c.1115C>T variants for PSTPIP1 and c.598G>A variant for *PPP1R32* into the genome. In short, endogenous PSTPIP1 and PPP1R32 proteins are still synthesized by the cells. So, we could not speculate the western blot results efficiently whether these variants have an effect on inflammasome activation or not.

Hence, further studies are needed for better understanding the effect and role of these three variants (c.682C>T and c.1115C>T for *PSTPIP1* and c.598G>A for *PPP1R32*) in the inflammasome pathways.

6. REFERENCES

1. Hoffman HM, Broderick L. The role of the inflammasome in patients with autoinflammatory diseases. Journal of Allergy and Clinical Immunology. 2016 Jul 1;138(1):3–14.

2. Georgin-Lavialle S, Fayand A, Rodrigues F, Bachmeyer C, Savey L, Grateau G. Autoinflammatory diseases: State of the art. Presse Med. 2019 Feb 1;48(1):e25–48.

3. Gurung P, Kanneganti TD. Autoinflammatory Skin Disorders: The Inflammasome in Focus. Trends Mol Med. 2016 Jul 1;22(7):545–64.

4. Krainer J, Siebenhandl S, Weinhäusel A. Systemic autoinflammatory diseases. J Autoimmun. 2020 May 1;109:102421.

5. Schnappauf O, Chae JJ, Kastner DL, Aksentijevich I. The Pyrin Inflammasome in Health and Disease. Front Immunol. 2019 Aug 7;10:1745.

6. Renauer P, Sawalha AH. The genetics of Takayasu arteritis. Presse Med [Internet]. 2017 Jul 1 [cited 2023 Dec 31];46(7-8 2):e179. Available from: /pmc/articles/PMC5753771/

7. Edwards SC, McGinley AM, McGuinness NC, Mills KHG. γδ T Cells and NK Cells – Distinct Pathogenic Roles as Innate-Like Immune Cells in CNS Autoimmunity. Front Immunol [Internet]. 2015 [cited 2023 Dec 31];6(SEP). Available from: /pmc/articles/PMC4561808/

8. Immune complexes in Takayasu's arteritis. - PMC [Internet]. [cited 2023 Dec 31]. Available from: https://www.ncbi.nlm.nih.gov/pmc/articles/PMC1537391/

9. Miller D V., Maleszewski JJ. The pathology of large-vessel vasculitides. Clin Exp Rheumatol [Internet]. 2011 [cited 2023 Dec 31];29(1 SUPPL. 64). Available from: https://www.clinexprheumatol.org/abstract.asp?a=4835

10. Page loading - ClinicalKey [Internet]. [cited 2023 Dec 31]. Available from: https://www.clinicalkey.com/#!/content/playContent/1-s2.0-S0889857X07000506?returnurl=https:%2F%2Flinkinghub.elsevier.com%2Fretrieve%2Fpii%2FS0889857X07000506%3Fshowall%3Dtrue&referrer=https:%2F%2Fpubmed.ncbi.nlm.nih.gov%2F

11. Brunner J, Feldman BM, Tyrrell PN, Kuemmerle-Deschner JB, Zimmerhackl LB, Gassner I, et al. Takayasu arteritis in children and adolescents. Rheumatology [Internet]. 2010 Oct 1 [cited 2023 Dec 31];49(10):1806–14. Available from: https://dx.doi.org/10.1093/rheumatology/keq167

12. Gornik HL, Creager MA. Aortitis. Circulation [Internet]. 2008 Jun 6 [cited 2023 Dec 31];117(23):3039. Available from: /pmc/articles/PMC2759760/

13. Jain S, Sharma N, Singh S, Bali HK, Kumar L, Sharma BK. Takayasu Arteritis in children and young Indians. Int J Cardiol. 2000 Aug 31;75(SUPPL. 1):S153–7.

14. Vaideeswar P, Deshpande JR. Pathology of Takayasu arteritis: A brief review. Ann Pediatr Cardiol [Internet]. 2013 Jan [cited 2023 Dec 31];6(1):52. Available from: /pmc/articles/PMC3634248/

15. Weiss PF. Pediatric Vasculitis. Pediatr Clin North Am [Internet]. 2012 Apr [cited 2023 Dec 31];59(2):407. Available from: /pmc/articles/PMC3348547/

16. Aeschlimann FA, Twilt M, Yeung RSM. Childhood-onset Takayasu Arteritis. Eur J Rheumatol [Internet]. 2020 Feb 3 [cited 2023 Dec 31];7(Suppl 1):S58. Available from: /pmc/articles/PMC7004266/

17. Lim AY, Lee GY, Jang SY, Gwag HB, Choi SH, Jeon ES, et al. Gender differences in clinical and angiographic findings of patients with Takayasu arteritis. Clin Exp Rheumatol [Internet]. 2015 Mar 1 [cited 2023 Dec 31];33(2). Available from: https://www.clinexprheumatol.org/abstract.asp?a=8973

18. Alnabwani D, Patel P, Kata P, Patel V, Okere A, Cheriyath P. The Epidemiology and Clinical Manifestations of Takayasu Arteritis: A Descriptive Study of Case Reports. Cureus [Internet]. 2021 Sep 15 [cited 2023 Dec 31];13(9). Available from: /pmc/articles/PMC8519497/

19. Onen F, Akkoc N. Epidemiology of Takayasu arteritis. Presse Med. 2017 Jul 1;46(7–8):e197–203.

20. Birlik M, Kücükyavas Y, Aksu K, Solmaz D, Can G, Taylan A, et al. Epidemiology of Takayasu's arteritis in Turkey. Clin Exp Rheumatol [Internet]. 2016 [cited 2023 Dec 31];34:S33–9. Available from: https://www.clinexprheumatol.org/abstract.asp?a=9349

21. Saritas F, Donmez S, Direskeneli H, Pamuk ON. The epidemiology of Takayasu arteritis: a hospital-based study from northwestern part of Turkey. Rheumatol Int [Internet]. 2016 Jul 1 [cited 2023 Dec 31];36(7):911–6. Available from: https://link.springer.com/article/10.1007/s00296-016-3445-z

22. Zhang Z, Wang W, Zhou M, Lu PYJ, Li Y, Chen Y. An Observational Study of Sex Differences in Takayasu Arteritis in China: Implications for Worldwide Regional Differences. Ann Vasc Surg. 2020 Jul 1;66:309–17.

23. Rutter M, Bowley J, Lanyon PC, Grainge MJ. A systematic review and meta-analysis of the incidence rate of Takayasu arteritis. Rheumatology (Oxford) [Internet]. 2021 Nov 1 [cited 2023 Dec 31];60(11):4982. Available from: /pmc/articles/PMC8566298/

24. Keser G, Aksu K, Direskeneli H. Takayasu arteritis: an update. Turk J Med Sci [Internet]. 2018 Jan 1 [cited 2023 Dec 31];48(4):681–97. Available from: https://journals.tubitak.gov.tr/medical/vol48/iss4/1

25. Tombetti E, Mason JC. Takayasu arteritis: advanced understanding is leading to new horizons. Rheumatology [Internet]. 2019 Feb 1 [cited 2023 Dec 31];58(2):206–19. Available from: https://dx.doi.org/10.1093/rheumatology/key040

26. Shiina T, Hosomichi K, Inoko H, Kulski JK. The HLA genomic loci map: expression, interaction, diversity and disease. Journal of Human Genetics 2009 54:1 [Internet]. 2009 Jan 9 [cited 2023 Dec 31];54(1):15–39. Available from: https://www.nature.com/articles/jhg20085

27. Kobayashi Y, Numano F. 3. Takayasu Arteritis. Internal Medicine. 2002;41(1):44–6.

28. Saruhan-Direskeneli G, Hughes T, Aksu K, Keser G, Coit P, Aydin SZ, et al. Identification of Multiple Genetic Susceptibility Loci in Takayasu Arteritis. Am J Hum Genet [Internet]. 2013 Aug 8 [cited 2023 Dec 31];93(2):298. Available from: /pmc/articles/PMC3738826/

29. Terao C. Revisited HLA and non-HLA genetics of Takayasu arteritis—where are we? Journal of Human Genetics 2016 61:1 [Internet]. 2015 Jul 16 [cited 2023 Dec 31];61(1):27–32. Available from: https://www.nature.com/articles/jhg201587

30. Tamura N, Maejima Y, Matsumura T, Vega RB, Amiya E, Ito Y, et al. Single-Nucleotide Polymorphism of the MLX Gene Is Associated With Takayasu Arteritis. Circ Genom Precis Med [Internet]. 2018 Oct 1 [cited 2023 Dec 31];11(10):e002296. Available from: /pmc/articles/PMC6522131/

31. Renauer PA, Saruhan-Direskeneli G, Coit P, Adler A, Aksu K, Keser G, et al. Genome-wide association study identifies susceptibility loci in IL6, RPS9/LILRB3, and an intergenic locus on chromosome 21q22 in Takayasu's arteritis. Arthritis Rheumatol [Internet]. 2015 May 1 [cited 2023 Dec 31];67(5):1361. Available from: /pmc/articles/PMC4414813/

32. Uciechowski P, Dempke WCM. Interleukin-6: A Masterplayer in the Cytokine Network. Oncology [Internet]. 2020 Feb 26 [cited 2023 Dec 31];98(3):131–7. Available from: https://dx.doi.org/10.1159/000505099

33. Tanaka T, Narazaki M, Kishimoto T. IL-6 in Inflammation, Immunity, and Disease. Cold Spring Harb Perspect Biol [Internet]. 2014 Oct 1 [cited 2023 Dec 31];6(10):16295–6. Available from: /pmc/articles/PMC4176007/

34. Chen S, Wen X, Li J, Li Y, Li L, Tian X, et al. Association of FCGR2A/FCGR3A variant rs2099684 with Takayasu arteritis in the Han Chinese population. Oncotarget [Internet]. 2017 Mar 3 [cited 2023 Dec 31];8(10):17239. Available from: /pmc/articles/PMC5370036/

35. Yoshifuji H, Terao C, Terao C, Terao C. Roles of cytotoxic lymphocytes and MIC/LILR families in pathophysiology of Takayasu arteritis. Inflamm Regen [Internet]. 2020 Jun 2 [cited 2023 Dec 31];40(1):1–5. Available from: https://inflammregen.biomedcentral.com/articles/10.1186/s41232-020-00119-6

36. Arnaud L, Haroche J, Mathian A, Gorochov G, Amoura Z. Pathogenesis of Takayasu's arteritis: A 2011 update. Autoimmun Rev. 2011 Nov 1;11(1):61–7.

37. Mirault T, Guillet H, Messas E. Immune response in Takayasu arteritis. Presse Med. 2017 Jul 1;46(7–8):e189–96.

38. Serra R, Butrico L, Fugetto F, Chibireva MD, Malva A, De Caridi G, et al. Updates in Pathophysiology, Diagnosis and Management of Takayasu Arteritis. Ann Vasc Surg. 2016 Aug 1;35:210–25.

39. Espinoza JL, Ai S, Matsumura I. New Insights on the Pathogenesis of Takayasu Arteritis: Revisiting the Microbial Theory. Pathogens 2018, Vol 7, Page 73 [Internet]. 2018 Sep 6 [cited 2023 Dec 31];7(3):73. Available from: https://www.mdpi.com/2076-0817/7/3/73/htm

40. Bhandari S, Butt SRR, Ishfaq A, Attaallah MH, Ekhator C, Nagaraj RH, et al. Pathophysiology, Diagnosis, and Management of Takayasu Arteritis: A Review of Current Advances. Cureus [Internet]. 2023 Jul 29 [cited 2023 Dec 31];15(7). Available from: /pmc/articles/PMC10386905/

41. Arnaud L, Haroche J, Toledano D, Cacoub P, Mathian A, Costedoat-Chalumeau N, et al. Cluster analysis of arterial involvement in Takayasu arteritis reveals symmetric extension of the lesions in paired arterial beds. Arthritis Rheum [Internet]. 2011 Apr 1 [cited 2023 Dec 31];63(4):1136–40. Available from: https://onlinelibrary.wiley.com/doi/full/10.1002/art.30240

42. Yunna C, Mengru H, Lei W, Weidong C. Macrophage M1/M2 polarization. Eur J Pharmacol. 2020 Jun 15;877:173090.

43. Bajocchi G, Cavazza A. Histopathology of vasculitis. Reumatismo [Internet]. 2018 Oct 3 [cited 2023 Dec 31];70(3):155–64. Available from: https://reumatismo.org/index.php/reuma/article/view/1096

44. Pugh D, Karabayas M, Basu N, Cid MC, Goel R, Goodyear CS, et al. Large vessel vasculitis. Nat Rev Dis Primers [Internet]. 2022 Jan 1 [cited 2023 Dec 31];7(1):93. Available from: /pmc/articles/PMC9115766/

45. Pathogenesis of Takayasu's arteritis - PubMed [Internet]. [cited 2023 Dec 31]. Available from: https://pubmed.ncbi.nlm.nih.gov/11783607/

46. Deng J, Younge BR, Olshen RA, Goronzy JJ, Weyand CM. Th17 and Th1 T-cell responses in Giant Cell Arteritis. Circulation [Internet]. 2010 Feb 2 [cited 2023 Dec 31];121(7):906. Available from: /pmc/articles/PMC2837465/

47. Shohat M, Halpern GJ. Familial Mediterranean fever—A review. Genetics in Medicine. 2011 Jun 1;13(6):487–98.

48. Tufan A, Lachmann HJ. Familial Mediterranean fever, from pathogenesis to treatment: a contemporary review. Turk J Med Sci [Internet]. 2020 [cited 2023 Dec 31];50(7):1591. Available from: /pmc/articles/PMC7672358/

49. Alghamdi M. Familial Mediterranean fever, review of the literature. Clin Rheumatol [Internet]. 2017 Aug 1 [cited 2023 Dec 31];36(8):1707–13. Available from: https://link.springer.com/article/10.1007/s10067-017-3715-5

50. Petrushkin H, Stanford M, Fortune F, Jawad AS. Clinical Review: Familial Mediterranean Fever—An Overview of Pathogenesis, Symptoms, Ocular Manifestations, and Treatment. Ocul Immunol Inflamm [Internet]. 2016 Jul 3 [cited 2023 Dec 31];24(4):422–30. Available from: https://www.tandfonline.com/doi/abs/10.3109/09273948.2015.1010012

51. Twig G, Livneh A, Vivante A, Afek A, Shamiss A, Derazne E, et al. Mortality risk factors associated with familial Mediterranean fever among a cohort of 1.25 million adolescents. Ann Rheum Dis [Internet]. 2014 Apr 1 [cited 2023 Dec 31];73(4):704–9. Available from: https://ard.bmj.com/content/73/4/704

52. Ahbap E, Kara E, Sahutoglu T, Basturk T, Koc Y, Sakaci T, et al. Outcome of 121 patients with renal amyloid a amyloidosis. J Res Med Sci [Internet]. 2014 [cited 2023 Dec 31];19(7):644. Available from: /pmc/articles/PMC4214024/

53. Bashardoust B. Familial Mediterranean fever; diagnosis, treatment, and complications. J Nephropharmacol [Internet]. 2015 [cited 2023 Dec 31];4(1):5. Available from: /pmc/articles/PMC5297479/

54. Ben-Chetrit E, Touitou I. Familial Mediterranean Fever in the World. Arthritis Care Res (Hoboken) [Internet]. 2009 Oct 15 [cited 2023 Dec 31];61(10):1447–53. Available from: https://onlinelibrary.wiley.com/doi/full/10.1002/art.24458

55. Migita K, Izumi Y, Jiuchi Y, Iwanaga N, Kawahara C, Agematsu K, et al. Familial Mediterranean fever is no longer a rare disease in Japan. Arthritis Res Ther [Internet]. 2016 Jul 30 [cited 2023 Dec 31];18(1):1–10. Available from: https://arthritis-research.biomedcentral.com/articles/10.1186/s13075-016-1071-5

56. Familial Mediterranean fever: Epidemiology, genetics, and pathogenesis - UpToDate [Internet]. [cited 2023 Dec 31]. Available from: https://www.uptodate.com/contents/familial-mediterranean-fever-epidemiology-genetics-and-pathogenesis

57. Sarı İ, Birlik M, Kasifoğlu T. Familial Mediterranean fever: An updated review. Eur J Rheumatol [Internet]. 2014 Mar 7 [cited 2023 Dec 31];1(1):21. Available from: /pmc/articles/PMC5042258/

58. Tunca M, Ozdogan H, Kasapcopur O, Yalcinkaya F, Ozen S, Topaloglu R, et al. Familial Mediterranean Fever (FMF) in Turkey: Results of a nationwide multicenter study. Medicine [Internet]. 2005 Jan 1 [cited 2023 Dec 31];84(1):1–11. Available from: https://journals.lww.com/md-journal/fulltext/2005/01000/familial_mediterranean_fever__fmf__in_turkey_.1.aspx

59. Aksentijevich I, Centola M, Deng Z, Sood R, Balow J, Wood G, et al. Ancient Missense Mutations in a New Member of the RoRet Gene Family Are Likely to Cause Familial Mediterranean Fever. Cell. 1997 Aug 22;90(4):797–807.

60. Bernot A, Clepet C, Dasilva C, Devaud C, Petit JL, Caloustian C, et al. A candidate gene for familial Mediterranean fever. Nature Genetics 1997 17:1 [Internet]. 1997 [cited 2023 Dec 31];17(1):25–31. Available from: https://www.nature.com/articles/ng0997-25

61. Touitou I. The spectrum of Familial Mediterranean Fever (FMF) mutations. European Journal of Human Genetics 2001 9:7 [Internet]. 2001 Jul 18 [cited 2023 Dec 31];9(7):473–83. Available from: https://www.nature.com/articles/5200658

62. Ben-Zvi I, Herskovizh C, Kukuy O, Kassel Y, Grossman C, Livneh A. Familial Mediterranean fever without MEFV mutations: A case-control study. Orphanet J Rare Dis [Internet]. 2015 Mar 25 [cited 2023 Dec 31];10(1):1–6. Available from: https://ojrd.biomedcentral.com/articles/10.1186/s13023-015-0252-7

63. Olgun A, Akman S, Kurt I, Tuzun A, Kutluay T. MEFV mutations in familial Mediterranean fever: Association of M694V homozygosity with arthritis. Rheumatol Int [Internet]. 2005 May 15 [cited 2023 Dec 31];25(4):255–9. Available from: https://link.springer.com/article/10.1007/s00296-003-0433-x

64. Aydın F, Çakar N, Özçakar ZB, Uncu N, Başaran Ö, Özdel S, et al. Clinical features and disease severity of Turkish FMF children carrying E148Q mutation. J Clin Lab Anal [Internet]. 2019 May 1 [cited 2023 Dec 31];33(4). Available from: /pmc/articles/PMC6528560/

65. Tirosh I, Yacobi Y, Vivante A, Barel O, Ben-Moshe Y, Erez Granat O, et al. Clinical significance of E148Q heterozygous variant in paediatric familial Mediterranean fever. Rheumatology [Internet]. 2021 Nov 3 [cited 2023 Dec 31];60(11):5447–51. Available from: https://dx.doi.org/10.1093/rheumatology/keab128

66. Cekin N, Akyurek ME, Pinarbasi E, Ozen F. MEFV mutations and their relation to major clinical symptoms of Familial Mediterranean Fever. Gene. 2017 Aug 30;626:9–13.

67. Paut IK, Dubuc M, Sportouch J, Minodier P, Garnier JM, Touitou I. Phenotype–genotype correlation in 91 patients with familial Mediterranean fever reveals a high frequency of cutaneomucous features. Rheumatology [Internet]. 2000 Nov 1 [cited 2023 Dec 31];39(11):1275–9. Available from: https://dx.doi.org/10.1093/rheumatology/39.11.1275

68. Booty MG, Jae JC, Masters SL, Remmers EF, Barham B, Le JM, et al. Familial mediterranean fever with a single MEFV mutation: Where is the second hit? Arthritis Rheum [Internet]. 2009 Jun 1 [cited 2023 Dec 31];60(6):1851–61. Available from: https://onlinelibrary.wiley.com/doi/full/10.1002/art.24569

69. Zekry ME, Sallam AAM, AbdelHamid SG, Zarouk WA, El-Bassyouni HT, El-Mesallamy HO. Genetic and Epigenetic Regulation of MEFV Gene and Their Impact on Clinical Outcome in Auto-Inflammatory Familial Mediterranean Fever Patients. Curr Issues Mol Biol [Internet]. 2023 Jan 1 [cited 2023 Dec 31];45(1):721. Available from: /pmc/articles/PMC9857527/

70. Accetturo M, D'Uggento AM, Portincasa P, Stella A. Improvement of MEFV gene variants classification to aid treatment decision making in familial Mediterranean fever. Rheumatology [Internet]. 2020 Apr 1 [cited 2023 Dec 31];59(4):754–61. Available from: https://dx.doi.org/10.1093/rheumatology/kez332

71. Seshadri S, Duncan MD, Hart JM, Gavrilin MA, Wewers MD. Pyrin Levels in Human Monocytes and Monocyte-Derived Macrophages Regulate IL-1β Processing and Release. The Journal of Immunology [Internet]. 2007 Jul 15 [cited 2023 Dec 31];179(2):1274–81. Available from: https://dx.doi.org/10.4049/jimmunol.179.2.1274

72. Heilig R, Broz P. Function and mechanism of the pyrin inflammasome. Eur J Immunol [Internet]. 2018 Feb 1 [cited 2023 Dec 31];48(2):230–8. Available from: https://onlinelibrary.wiley.com/doi/full/10.1002/eji.201746947

73. Galliher-Beckley AJ, Lan LQ, Aono S, Wang L, Shi J. Caspase-1 activation and mature interleukin-1β release are uncoupled events in monocytes. World J Biol Chem [Internet]. 2013 May 5 [cited 2023 Dec 31];4(2):30. Available from: /pmc/articles/PMC3652645/

74. Akbaba TH, Akkaya-Ulum YZ, Demir S, Ozen S, Balci-Peynircioglu B. The pyrin inflammasome aggravates inflammatory cell migration in patients with familial Mediterranean fever. Pediatric Research 2021 91:6 [Internet]. 2021 May 7 [cited 2023 Dec 31];91(6):1399–404. Available from: https://www.nature.com/articles/s41390-021-01559-7

75. Bergsbaken T, Fink SL, Cookson BT. Pyroptosis: host cell death and inflammation. Nat Rev Microbiol [Internet]. 2009 [cited 2023 Dec 31];7(2):99. Available from: /pmc/articles/PMC2910423/

76. Dedeoglu F, Kim S. Autoinflammatory Disorders. Pediatric Allergy: Principles and Practice Expert Consult: Second Edition. 2010 Jan 1;232–9.

77. Manso JA, Marcos T, Ruiz-Martín V, Casas J, Alcón P, Sánchez Crespo M, et al. PSTPIP1-LYP phosphatase interaction: structural basis and implications for autoinflammatory disorders. Cellular and Molecular Life Sciences [Internet]. 2022 Feb 1 [cited 2023 Dec 31];79(2):1–17. Available from: https://link.springer.com/article/10.1007/s00018-022-04173-w

78. Davidson D, Veillette A. PTP-PEST, a scaffold protein tyrosine phosphatase, negatively regulates lymphocyte activation by targeting a unique set of substrates. EMBO J [Internet]. 2001 Jul 7 [cited 2023 Dec 31];20(13):3414. Available from: /pmc/articles/PMC125513/

79. Önen MÖ, Onat UI, Uğurlu S, Timuçin AC, Öz Arslan D, Everest E, et al. Detection of a rare variant in PSTPIP1 through three generations in a family with an initial diagnosis of FMF/MKD-overlapping phenotype. Rheumatology [Internet]. 2023 Sep 1 [cited 2023 Dec 31];62(9):3188–96. Available from: https://dx.doi.org/10.1093/rheumatology/kead044

80. de Jesus AA, Ferguson PJ, Goldbach-Mansky R. Classic Autoinflammatory Diseases: Monogenic Autoinflammatory Diseases Caused by Defects in CIAS1, MEFV, TNFRSF1A, MVK, and PSTPIP1. Stiehm's Immune Deficiencies. 2014 Jan 1;517–50.

81. Akkaya-Ulum YZ, Balci-Peynircioglu B, Purali N, Yilmaz E. Pyrin–PSTPIP1 colocalises at the leading edge during cell migration. Cell Biol Int [Internet]. 2015 Dec 1 [cited 2023 Dec 31];39(12):1384–94. Available from: https://onlinelibrary.wiley.com/doi/full/10.1002/cbin.10514

82. El-Shebiny EM, Zahran ES, Shoeib SA, Habib ES. Bridging autoinflammatory and autoimmune diseases. The Egyptian Journal of Internal Medicine 2021 33:1 [Internet]. 2021 Mar 29 [cited 2023 Dec 31];33(1):1–9. Available from: https://ejim.springeropen.com/articles/10.1186/s43162-021-00040-5

83. Batlle-Masó L, Mensa-Vilaró A, Solís-Moruno M, Marquès-Bonet T, Arostegui JI, Casals F. Genetic diagnosis of autoinflammatory disease patients using clinical exome sequencing. Eur J Med Genet. 2020 May 1;63(5):103920.

84. Miner JJ, Fitzgerald KA. A path towards personalized medicine for autoinflammatory and related diseases. Nature Reviews Rheumatology 2023 19:3 [Internet]. 2023 Feb 7 [cited 2023 Dec 31];19(3):182–9. Available from: https://www.nature.com/articles/s41584-022-00904-2

85. Karacan I, Uğurlu S, Tolun A, Turanli ET, Özdoğan H. Other autoinflammatory disease genes in an FMF-prevalent population: A homozygous MVK mutation and a heterozygous TNFRSF1A mutation in two different Turkish families with clinical FMF. Clin Exp Rheumatol [Internet]. 2017 [cited 2024 Jan 2];35:S75–81. Available from: https://www.clinexprheumatol.org/abstract.asp?a=11822

86. Jo EK, Kim JK, Shin DM, Sasakawa C. Molecular mechanisms regulating NLRP3 inflammasome activation. Cell Mol Immunol [Internet]. 2016 Mar 1 [cited 2024 Jan 2];13(2):148. Available from: /pmc/articles/PMC4786634/

87. Chae JJ, Komarow HD, Cheng J, Wood G, Raben N, Liu PP, et al. Targeted Disruption of Pyrin, the FMF Protein, Causes Heightened Sensitivity to Endotoxin and a Defect in Macrophage Apoptosis. Mol Cell. 2003 Mar 1;11(3):591–604.

88. Sag E, Bilginer Y, Ozen S. Autoinflammatory Diseases with Periodic Fevers. Curr Rheumatol Rep [Internet]. 2017 Jul 1 [cited 2024 Jan 2];19(7):1–10. Available from: https://link.springer.com/article/10.1007/s11926-017-0670-8

89. Holzinger D, Roth J. PAPA Syndrome and the Spectrum of PSTPIP1-Associated Inflammatory Diseases. Auto-Inflammatory Syndromes: Pathophysiology, Diagnosis, and Management [Internet]. 2019 Jan 1 [cited 2024 Jan 2];39–59. Available from: https://link.springer.com/chapter/10.1007/978-3-319-96929-9_4

90. Other autoinflammatory disease genes in an FMF-prevalent population: a homozygous MVK mutation and a novel heterozygous TNFRSF1A mutation in two different Turkish families with clinical FMF - PubMed [Internet]. [cited 2024 Feb 13]. Available from: https://pubmed.ncbi.nlm.nih.gov/29148404/

91. Yu JW, Fernandes-Alnemri T, Datta P, Wu J, Juliana C, Solorzano L, et al. Pyrin activates the ASC pyroptosome in response to engagement by autoinflammatory PSTPIP1 mutants. Mol Cell [Internet]. 2007 Oct 10 [cited 2024 Feb 13];28(2):214. Available from: /pmc/articles/PMC2719761/

92. Borgia P, Papa R, D'Alessandro M, Caorsi R, Piaggio G, Angeletti A, et al. Kidney Involvement in PSTPIP1 Associated Inflammatory Diseases (PAID): A Case Report and Review of the Literature. Front Med (Lausanne) [Internet]. 2021 Oct 29 [cited 2024 Feb 13];8:759092. Available from: /pmc/articles/PMC8586089/

APPENDIX A

Chemicals	**Supplier Company, Catalog Number**
1 kb DNA ladder	ThermoScientific, 10787018
100 bp DNA ladder	ThermoScientific, 15628019
40% Acrylamide	BIORAD, 1610140
50x TAE Buffer	GeneMark, GB01-1
6x Gel loading solution	ThermoScientific, R061 1
Absolute Ethanol	ISOLAB, 920.026.2500
Agarose	BIOMAX, HS8000
Ampicillin	SERVA, 13398.01
Anti-mouse antibody	Cell Signaling Technology, 7076S
Anti-rabbit antibody	Cell Signaling Technology, 7074S
APS	AppliChem, A2941,0100
Adeonsine triphosphate (ATP)	Santa Cruz, 987-65-5
B-mercaptoethanol	BIOSHOP, MER002
Bovine Serum Albumin	Capricorn, BSA-1U
Chloroform	Sigma-Aldrich, 67-66-3
DMSO	ThermoScientific, F-515
DNA polymerase	ThermoScientific, EP0401
dNTP	QIAGEN, 201912
DPBS	Gibco, 14190144
ECL	ThermoScientific, 32209

EDTA	BIOSHOP, 6381-92-6
FBS	Biowest, S181H
GAPDH Antibody	Cell Signaling Technology, 5174S
Genopure Midi Kit	Roche, 3143414001
Glycerol	ISOLAB, 56-81-5
Glycine	AFG Scientific, 336599
HCI	Sigma-Aldrich, 7647-01-0
HEPES	EuroClone ,ECM0180D
High Fidelity DNA polymerase	NEB, M0491S
L-glutamine	Sigma-Aldrich, G8540
Isopropanol	ISOLAB, 961.028.2501
LB agar	Biolife, 4110302
LB broth	Bioshop, LBL407
LipoFectMax 3000	ABP Biosciences, FP319
Lipopolysaccharide (500X)	ThermoScientific, 00-4976-93
Methanol	ISOLAB, 947.046.2500
NaCI	ISOLAB, 969.036.1000
NaOH	Sigma-Aldrich, 06203
Opti-MEM (1X)	Gibco, 31985070
Penicillin/Streptomycin	Sigma-Aldrich, p4333
PBS tablet	Bioshop, PBS404
Protease Inhibitor Cocktail	BOSTER, AR1182-A
Pierce BCA Protein Assay Kit	ThermoScientific, 23225

HRP-conjugated Mouse anti DYK-Tag mAb	ABclonal, AE024
PPP1R32 cDNA ORF clone	GenScript, OHu55642
PSTPIP1 Antibody	Santa Cruz, sc-390727
PSTPIP1 (NM_003978) Human Untagged Clone	ORIGENE, SC322259
RPMI-1640	PAN Biotech, P04-18500
SDS	ISOLAB, 915.02P.0050 -
TEMED	Bioshop, TEM001.R
Prestained protein ladder	ThermoScientific, 26619
Trizma Base	Sigma-Aldrich, 77-86-1
Triton-X	BioShop, TRX777
TWEEN 20	Sigma-Aldrich, P1379

APPENDIX B

Equipments	**Supplier Company, Catalog Number**
0.2 ml PCR tube	ThermoScientific, AB0620
1.5 ml Microcentrifuge tube	ISOLAB, 078.05.022
100 mm Petri Dish	ISOLAB, 081.01.100
12 well Cell Culture Plate	TPP, 92112
15 ml Centrifuge Tube	ISOLAB, 079.08.015B
50 ml Centrifuge Tube	ISOLAB, 079.08.015L
96 well Microplate	TPP, 92148
Allegra X-30R Centrifuge (Refrigerated)	Beckman Coulter, A99471
Autoclave	NUVE, NC 90M
Benchtop Incubated Orbital Shaker	INOVIA Technology, TS-1
C1000 Touch Thermal Cycler	BIORAD, 1851196
ChemiDoc MP Imaging System	BIORAD, 12003154
CO_2 Incubator	ThermoScientific, 381
EVOS^{TM} M5000 Imaging System	ThermoScientific, AMF5000
Freezer (-80□C)	ARCTIKO
Horizantal Electrophoresis System	BIORAD, 1704468
Inverted Microscope	ZEISS
Laminar Flow Hood	ThermoScientific, KS15
Magnetic Stirrer	VELP SCIENTIFICA, A00000356
Microplate Reader	BioTek, 800TS

Microwave Oven	Arçelik, MD574
Mini Centrifuge	OHAUS, FC5306
Mini Orbital Shaker	Stuart, SSM1
Mini Trans-Blot Module	BIORAD, 1703930
NanoDrop ONE	ThermoScientific, 701-058112
Precision Water Bath	ThermoScientific, TSGP28
Protein Electrophoresis System	BIORAD, 1658004
Refrigerator (+4□C)	ARCTIKO
Refrigerator (-20□C)	ARCTIKO
Sample Mixer	Biosan, RS-24
Syringe Filter (0.22 µm)	ISOLAB, 094.07.002
T100 Thermal Cycler	BIORAD, 1861096
T25 Cell Culture Flask	TPP, 90025
T75 Cell Culture Flask	TPP, 90075
Thermal Shaking Incubator	ThermoScientific, 11-675-204
Vortex	ThermoScientific, 16534622

APPENDIX C

100 bp DNA Ladder

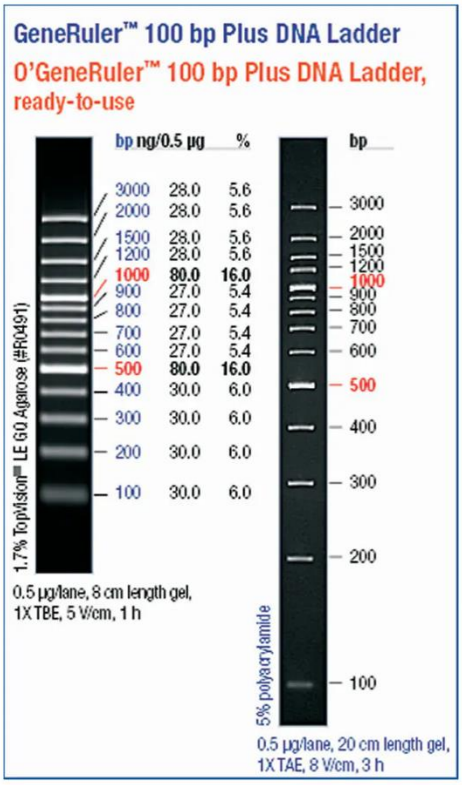

APPENDIX D

1 kb DNA Ladder

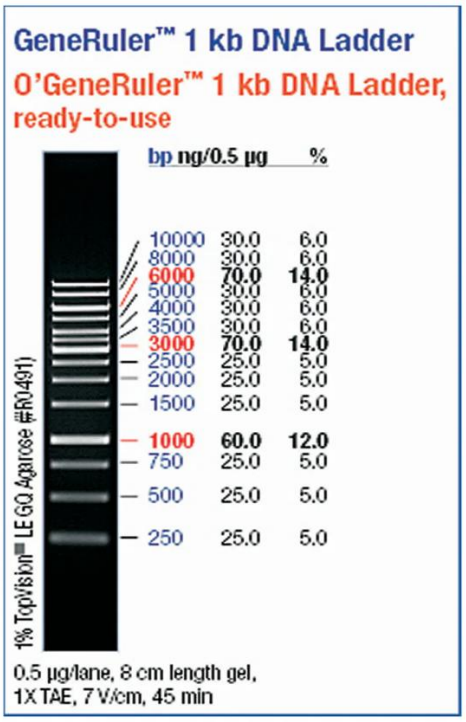

APPENDIX E

Pageruler Plus Prestained Protein Ladder

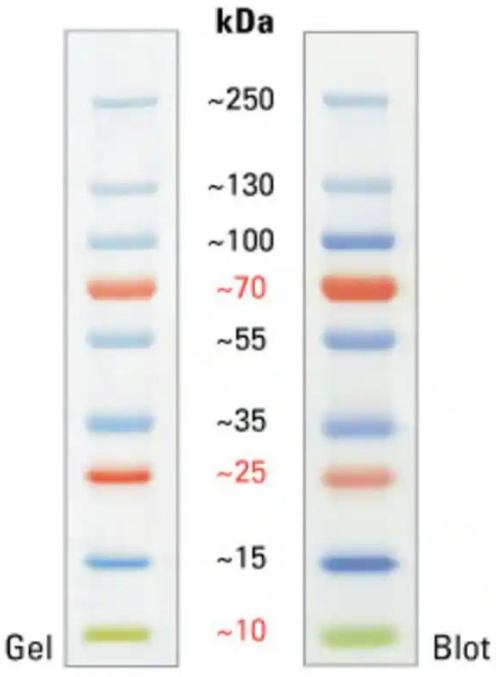

7. CURRICULUM VITAE